Inorganic Chemistry
Article

Inorg. Chem. **2010**, *49*, 1535–1550 **1535**
DOI: 10.1021/ic9019553

Series of 2D and 3D Coordination Polymers Based on 1,2,3,4-Benzenetetracarboxylate and N-Donor Ligands: Synthesis, Topological Structures, and Photoluminescent Properties

Lai-Ping Zhang, Jian-Fang Ma,* Jin Yang,* Yuan-Yuan Pang, and Ji-Cheng Ma

Key Lab for Polyoxometalate Science, Department of Chemistry, Northeast Normal University, Changchun 130024, People's Republic of China

Received October 4, 2009

Nine new coordination polymers, namely, $[Mn_2(L)(H_2O)_4]\cdot H_2O$ (**1**), $[Cd(L)_{0.5}(H_2O)]$ (**2**), $[Zn_5(L)_2(\mu_3\text{-}O)_2(H_2O)_4]\cdot 2H_2O$ (**3**), $[Zn_4(L)_2(\mu_3\text{-}O)_2][Zn(H_2O)_5]\cdot 2H_2O$ (**4**), $[Zn_2(L)(biim\text{-}4)_{0.5}(H_2O)_3]\cdot H_2O$ (**5**), $[Cd_2(L)(bpy)(H_2O)]\cdot 2H_2O\cdot 0.5(CH_3CH_2OH)$ (**6**), $[Cu_2(H_2L)_2(bpy)_2]$ (**7**), $[Cu_2(L)(bpy)(H_2O)]$ (**8**), and $[Cu_2(L)(bpy)_{1.5}(H_2O)_{2.5}]$ (**9**), where H_4L = 1,2,3,4-benzenetetracarboxylic acid, biim-4 = 1,1′-(1,4-butanediyl)bis(imidazole), and bpy = 4,4′-bipyridine, have been synthesized under hydrothermal conditions. Compound **1** displays a rare trinodal (3,4,7)-connected $(4^2\cdot 6)(4^5\cdot 6)(4^7\cdot 6^8\cdot 8^6)$ topology. **2** possesses an α-Po net. **3** is a novel 3D framework based on pentanuclear Zn^{II} clusters. By adjustment of the pH values of the reaction mixture of **3** with a Na_2CO_3 solution, a structurally different compound, **4**, was obtained, which exhibits a 3D porous framework with the $[Zn(H_2O)_6]^{2+}$ cations located in the channels. **5** is an unusual example of a trinodal (3,5)-connected network with a Schläfli symbol of $(4^2\cdot 6)(6^2\cdot 8)(4^2\cdot 6^2\cdot 8^5\cdot 10)$, whereas **6**, containing tetranuclear Cd^{II} clusters, shows a rare (4,6)-connected $(4^4\cdot 6^2)_2(4^4\cdot 6^{10}\cdot 8)$ topology. **7** exhibits a unique polythreading network, while **8** displays a scarce trinodal (3,4,5)-connected self-penetrating network. In comparison with **8**, the chiral compound **9** possesses an unprecedented tetranodal (2,4)-connected $(7)(7^5\cdot 11)(6^2\cdot 7^3\cdot 8)_2(6\cdot 7^4\cdot 10)_2$ topology. The effects of the carboxylate ligands, the pH values, the reaction temperatures, the central metals, and the neutral ligands were elucidated. The IR spectra, thermogravimetric analysis, and luminescent properties for the compounds were also investigated.

Introduction

The design and synthesis of metal−organic coordination polymers are of great current interest not only for their potential applications in sorption, electrical conductivity, smart optoelectronics, magnetism, and catalysis but also for their intriguing variety of architectures and fascinating new topologies.[1,2] Up to date, a number of examples have evidenced that topological types unprecedented in inorganic compounds and minerals can also be observed within metal−organic coordination polymers.[3] The topological analysis of metal−organic frameworks (MOFs) has been a topical research area not only for the importance of simplifying complicated frameworks of coordination polymers but also for the instructive role in the rational design of some predicted functional materials.[4] So far, numerous reported coordination polymers with mineral topologies, including $CdSO_4$ (**cds**), NbO (**nbo**), Pt_3O_4 (**pto**), pyrite (**pyr**), quartz (**qtz**), rutile (**rto**), diamond (**dia**), and sodalite (**sod**), have provided experimental examples of these theoretical topologies.[3a,5,6] As a result, the design and construction of diverse topological networks have received much attention.[7]

Recently, entanglement systems have attracted chemical interest because of their intriguing topological properties.[8] Among different types of entanglements, such as

*To whom correspondence should be addressed. E-mail: jianfangma@yahoo.com.cn (J.F.M.), yangjinnenu@yahoo.com.cn (J.Y.). Fax: +86-431-85098620.

(1) (a) Holliday, B. J.; Mirkin, C. A. *Angew. Chem., Int. Ed.* **2001**, *40*, 2022. (b) Leininger, S.; Olenyuk, B.; Stang, P. J. *Chem. Rev.* **2000**, *100*, 853. (c) Hosseini, M. W. *Acc. Chem. Res.* **2005**, *38*, 313. (d) Liu, J.-Q.; Wang, Y.-Y.; Ma, L.-F.; Zhong, F.; Zeng, X.-R.; Wu, W.-P.; Shi, Q.-Z. *Inorg. Chem. Commun.* **2007**, *10*, 979. (e) Steel, P. J. *Acc. Chem. Res.* **2005**, *38*, 243. (f) Brammer, L. *Chem. Soc. Rev.* **2004**, *33*, 476. (g) Seidel, S. R.; Stang, P. J. *Acc. Chem. Res.* **2002**, *35*, 972. (h) Caulder, D. L.; Raymond, K. N. *Acc. Chem. Res.* **1999**, *32*, 975. (i) Cui, Y. S.; Lee, J.; Lin, W. *J. Am. Chem. Soc.* **2003**, *125*, 6014. (j) Knof, U.; Zelewsky, A. *Angew. Chem., Int. Ed.* **1999**, *38*, 302.

(2) (a) Carlucci, L.; Ciani, G.; Proserpio, D. M.; Sironi, A. *J. Chem. Soc., Dalton Trans.* **1997**, 1801. (b) Khlobystov, A. N.; Blake, A. J.; Champness, N. R.; Lemenovskii, D. A.; Majouga, A. G.; Zyk, N. V.; Schröer, M. *Coord. Chem. Rev.* **2001**, *222*, 155. (c) Moulton, B.; Zaworotko, M. J. *Chem. Rev.* **2001**, *101*, 1629. (d) Zaworotko, M. J. *Chem. Commun.* **2001**, 1. (e) Yaghi, O. M.; O'Keeffe, M.; Ockwig, N. W.; Chae, H. K.; Eddaoudi, M.; Kim, J. *Nature* **2003**, *423*, 705.

(3) (a) Carlucci, L.; Ciani, G.; Macchi, P.; Proserpio, D. M. *Chem. Commun.* **1998**, 1837. (b) Abrahams, B. F.; Batten, S. R.; Grannas, M. J.; Hamit, H.; Hoskins, B. F.; Robson, R. *Angew. Chem., Int. Ed.* **1999**, *38*, 1475. (c) Lucia, C.; Gianfranco, C.; Davide, M. P.; Silvia, R. *J. Chem. Soc., Dalton Trans.* **2000**, 3821.

(4) (a) Wells, A. F. *Three-Dimensional Nets and Polyhedra*; Wiley: New York, 1977.(b) Natarajan, R.; Savitha, G.; Dominiak, P.; Wozniak, K.; Moorthy, J. N. *Angew. Chem., Int. Ed.* **2005**, *44*, 2115. (c) Robson, R. *J. Chem. Soc., Dalton Trans.* **2000**, 3735.

Published on Web 01/22/2010

polycatenation, polythreading, and polyknotting, interest in interpenetration and self-penetration (polyknotting) has increased rapidly because of their ordered polymeric networks, as well as fascinating topological and physical properties.[8b,9] Interpenetration occurs when two or more unconnected infinite networks penetrate through each other such that they cannot be separated without breaking bonds within the networks.[10] The large free voids in a single network may be the precondition for the formation of interpenetration. In comparison with the widely studied interpenetrating networks, the investigation of self-penetrating networks, in which the smallest topological circuits are passed through by rods of the same net, remains relatively less explored.[8b,10]

On the other hand, the construction of the MOFs can be influenced by many factors, such as the pH value of the solution, temperature, geometric requirements of the metal atoms, and ligands. Polycarboxylate anions, as good candidates for the construction of coordination polymers, have been well investigated by Yaghi et al.[11] So far, the benzenepolycarboxylate acids, such as 1,2,3-benzenetricarboxylic acid, 1,3,5-benzenecarboxylic acid, and 1,2,4,5-benzenetetracarboxylic acid, have been widely used in the construction of coordination polymers.[12] However, the new tetracarboxylate ligand 1,2,3,4-benzenetetracarboxylic acid (H_4L) has received less attention. Owing to the special arrangement of the four carboxylate groups, H_4L offers intriguing characteristics: (1) it can bridge the central metals to give a series of interesting structures through complete or partial deprotonation of its four carboxylate groups; (2) the adjacent arrangement of the four carboxylate groups, affording much stronger steric hindrance, prevents some of the carboxylate groups from lying in the same plane as the phenyl ring, and, thus, the carboxylate groups tend to connect the metal ions in different directions. On the basis of the above consideration, we synthesized nine coordination polymers containing L or H_2L^{2-} anions: $[Mn_2(L)(H_2O)_4]\cdot H_2O$ (**1**), $[Cd(L)_{0.5}(H_2O)]$ (**2**), $[Zn_5(L)_2(H_2O)_4]\cdot 2H_2O$ (**3**), $[Zn_4(L)_2(\mu_3\text{-}O)_2]$ $[Zn(H_2O)_5]\cdot 2H_2O$ (**4**), $[Zn_2(L5)(biim\text{-}4)_{0.5}(H_2O)_3]\cdot H_2O$ (**5**), $[Cd_2(L)(bpy)(H_2O)]\cdot 2H_2O\cdot 0.5(CH_3CH_2OH)$ (**6**), $[Cu_2(H_2L)_2(bpy)_2]$ (**7**), $[Cu_2(L)(bpy)(H_2O)]$ (**8**), and $[Cu_2(L)(bpy)_{1.5}(H_2O)_{2.5}]$ (**9**), where biim-4 = 1,1′-(1,4-butanediyl)bis(imidazole) and bpy = 4,4′-bipyridine (Scheme 1), by controlling the reaction temperature and pH value of the solution. The crystal structures as well as the topological analysis of these compounds, and the systematic description of the coordination modes of the polycarboxylate anions, will be discussed. The luminescent properties of compounds **2**−**6** were also investigated.

Scheme 1. Structures of the bpy (Top) and biim-4 (Bottom) Ligands

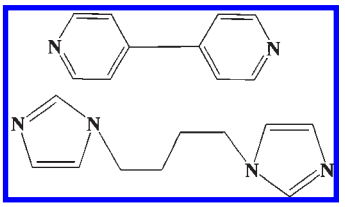

Experimental Section

General Characterization and Physical Measurements. All reagents and solvents were purchased from commercial sources and used as received. The C, H, and N elemental analysis was conducted on a Perkin-Elmer 240C elemental analyzer. Inductively coupled plasma (ICP) analysis was carried out on a Perkin-Elmer Optima 3300 DV spectrometer. The Fourier transform IR spectra were recorded from KBr pellets in the range 4000−400 cm^{-1} on a Mattson Alpha-Centauri spectrometer. Thermogravimetric analysis (TGA) was performed on a Perkin-Elmer TG-7 analyzer heated from 30 to 800 °C under nitrogen. The photoluminescent properties of the ligands and compounds were measured on a Perkin-Elmer LS55 spectrometer. The emission/excitation spectra and the lifetime were measured on an Edinburgh FLS-920 spectrophotometer equipped with a continuous Xe-900 xenon lamp and an nF900 ns flash lamp. biim-4 was synthesized in accordance with the procedure reported.[13]

Synthesis of $[Mn_2(L)(H_2O)_4]\cdot H_2O$ (1). To 10 mL of an ethanol−water [1:4 (v/v)] solution was added $Mn(CH_3COO)_2\cdot 4H_2O$ (49.0 mg, 0.20 mmol) and H_4L (25.4 mg, 0.10 mmol) with stirring at room temperature. After a few minutes, the cloudy solution was sealed in a Teflon reactor (15 mL), which was heated at 170 °C for 3 days and then cooled to room temperature at 10 °C·h^{-1}. Colorless crystals of **1** were collected in 55% yield [based on $Mn(CH_3COO)_2$]. ICP analysis of **1** gave the content of Mn as 24.55% (calcd 24.41%). Anal. Calcd for $C_{10}H_{12}Mn_2O_{13}$ (M_r = 450.08): C, 26.68; H, 2.69. Found: C, 26.42; H, 2.53. IR (cm^{-1}): 3420 (w), 1546 (m), 1374 (s), 1102 (m), 828 (w), 708 (w), 524 (m).

Synthesis of $[Cd(L)_{0.5}(H_2O)]$ (2). The preparation of **2** was similar to that of **1** except that $Cd(CH_3COO)_2\cdot 2H_2O$ was used in place of $Mn(CH_3COO)_2\cdot 4H_2O$. Colorless crystals of **2** were collected in 54% yield [based on $Cd(CH_3COO)_2$]. ICP analysis of **2** gave the content of Cd as 43.65% (calcd 44.00%). Anal. Calcd for $C_5H_3CdO_5$ (M_r = 255.47): C, 23.51; H, 1.18. Found: C, 23.66; H, 1.01. IR (cm^{-1}): 2981 (w), 1557 (s), 1467 (m), 1364 (s), 928 (w), 712 (m), 522 (m).

Synthesis of $[Zn_5(L)_2(\mu_3\text{-}O)_2(H_2O)_4]\cdot 2H_2O$ (3). The preparation of **3** was similar to that of **1** except that $Zn(CH_3COO)_2\cdot 2H_2O$ was used in place of $Mn(CH_3COO)_2\cdot 4H_2O$. The initial pH value for **3** was 3.2. Colorless crystals of **3** were collected in 48% yield [based on $Zn(CH_3COO)_2$]. ICP analysis of **3** gave the content of Zn as 33.58% (calcd 33.81%). Anal. Calcd for

(5) (a) Ockwig, N. W.; Delgado-Friedrichs, O.; O'Keeffe, M.; Yaghi, O. M. *Acc. Chem. Res.* **2005**, *38*, 176. (b) Wei, G.-H.; Yang, J.; Ma, J.-F.; Liu, Y.-Y.; Li, S.-L.; Zhang, L.-P. *Dalton Trans.* **2008**, 3080. (c) Power, K. N.; Hennigar, T. L.; Zaworotko, M. J. *Chem. Commun.* **1998**, 595. (d) Long, D.-L.; Blake, A. J.; Champness, N. R.; Schroder, M. *Chem. Commun.* **2000**, 1369. (e) Barnett, S. A.; Blake, A. J.; Champness, N. R.; Wilson, C. *Chem. Commun.* **2002**, 1640. (f) Moulton, B.; Abourahma, H.; Bradner, M. W.; Lu, J.; McManus, G. J.; Zaworotko, M. J. *Chem. Commun.* **2003**, 1342.

(6) (a) Eddaoudi, M.; Kim, J.; O'Keeffe, M.; Yaghi, O. M. *J. Am. Chem. Soc.* **2002**, *124*, 376. (b) Chen, B.; Fronczek, F. R.; Maverick, A. W. *Chem. Commun.* **2003**, 2166. (c) Sun, J. Y.; Weng, L. H.; Zhou, Y. M.; Chen, J. X.; Chen, Z. X.; Liu, Z. C.; Zhao, D. Y. *Angew. Chem., Int. Ed.* **2002**, *41*, 4471. (d) Zhang, J.; Kang, Y.; Zhang, R.-B.; Li, Z.-J.; Cheng, J.-K.; Yao, Y.-G. *CrystEngComm* **2005**, *7*, 177.

(7) Tong, M.-L.; Chen, X.-M.; Batten, S. R. *J. Am. Chem. Soc.* **2003**, *125*, 16170.

(8) (a) Carlucci, L.; Ciani, G.; Proserpio, D. M.; Rizzato, S. *CrystEngComm* **2003**, 190. (b) Carlucci, L.; Ciani, G.; Proserpio, D. M. *Coord. Chem. Rev.* **2003**, *246*, 247.

(9) Li, Z.-G.; Wang, G.-H.; Jia, H.-Q.; Hu, N.-H.; Xu, J.-W.; Batten, S. R. *CrystEngComm* **2008**, 983.

(10) (a) Batten, S. R.; Robson, R. *Angew. Chem., Int. Ed.* **1998**, *37*, 1460. (b) Batten, S. R. *CrystEngComm* **2001**, 67.

(11) (a) Yaghi, O. M.; Li, H.; Davis, C.; Richardson, D.; Groy, T. L. *Acc. Chem. Res.* **1998**, *31*, 474. (b) Chen, B.; Eddaoudi, M.; Reineke, T. M.; Kampf, J. W.; O'Keeffe, M.; Yaghi, O. M. *J. Am. Chem. Soc.* **2000**, *122*, 11559.

(12) (a) Gutschke, S. O. H.; Price, D. J.; Powell, A. K.; Wood, P. T. *Angew. Chem., Int. Ed.* **2001**, *40*, 1920. (b) Ghosh, S. K.; Bharadwaj, P. K. *Inorg. Chem.* **2004**, *43*, 5180. (c) Zhang, J.; Chen, Y.-B.; Chen, S.-M.; Li, Z.-J.; Cheng, J.-K.; Yao, Y.-G. *Inorg. Chem.* **2006**, *45*, 3161.

(13) Yang, J.; Ma, J.-F.; Liu, Y.-Y.; Li, S.-L.; Zheng, G.-L. *Eur. J. Inorg. Chem.* **2005**, 2174.

$C_{20}H_{16}Zn_5O_{24}$ (M_r = 967.18): C, 24.84; H, 1.67. Found: C, 24.69; H, 1.79. IR (cm^{-1}): 3386 (w), 3124 (m), 1615 (s), 1491 (s), 1374 (s), 1102 (m), 835 (w), 656 (m), 436 (w).

Synthesis of $[Zn_4(L)_2(\mu_3\text{-}O)_2][Zn(H_2O)_5]\cdot 2H_2O$ (4). The preparation of **4** was similar to that of **3** except that a Na_2CO_3 solution (0.2 mol·L^{-1}) was used to adjust the pH value to 4.5. Colorless crystals of **4** were collected in 52% yield [based on $Zn(CH_3COO)_2$]. ICP analysis of **4** gave the content of Zn as 32.92% (calcd 33.19%). Anal. Calcd for $C_{20}H_{18}Zn_5O_{25}$ (M_r = 985.20): C, 24.38; H, 1.84. Found: C, 24.50; H, 1.71. IR (cm^{-1}): 3480 (w), 3102 (w), 1635 (s), 1574 (w), 1370 (s), 1289 (m), 836 (m), 726 (s), 427 (w).

Synthesis of $[Zn_2(L)(biim\text{-}4)_{0.5}(H_2O)_3]\cdot H_2O$ (5). To 10 mL of an ethanol−water [1:4 (v/v)] solution was added $Zn(CH_3COO)_2\cdot 2H_2O$ (43.9 mg, 0.20 mmol), biim-4 (38.0 mg, 0.20 mmol), and H_4L (25.4 mg, 0.10 mmol) with stirring at room temperature. After a few minutes, the cloudy solution was sealed in a Teflon reactor (15 mL), which was heated at 170 °C for 3 days and then cooled to room temperature at 10 °C·h^{-1}. Colorless crystals of **5** were collected in 56% yield [based on $Zn(CH_3COO)_2$]. ICP analysis of **5** gave the content of Zn as 23.41% (calcd 23.86%). Anal. Calcd for $C_{15}H_{17}Zn_2N_2O_{12}$ (M_r = 548.05): C, 32.87; H, 3.13; N, 5.11. Found: C, 32.72; H, 3.32; N, 5.25. IR (cm^{-1}): 3284 (w), 3023 (w), 1635 (s), 1568 (m), 1374 (m), 1210 (m), 1022 (w), 835 (w), 725 (s), 430 (w).

Synthesis of $[Cd_2(L)(bpy)(H_2O)]\cdot 0.5EtOH\cdot 2H_2O$ (6). To 10 mL of an ethanol−water [1:4 (v/v)] solution was added $Cd(CH_3COO)_2\cdot 2H_2O$ (53.3 mg, 0.20 mmol), bpy (31.2 mg, 0.20 mmol), and H_4L (25.4 mg, 0.10 mmol) with stirring at room temperature. After a few minutes, the cloudy solution was sealed in a Teflon reactor (15 mL), which was heated at 170 °C for 3 days and then cooled to room temperature at 10 °C·h^{-1}. Colorless crystals of **6** were collected in 52% yield [based on $Cd(CH_3COO)_2$]. ICP analysis of **6** gave the content of Cd as 31.49% (calcd 31.74%). Anal. Calcd for $C_{21}H_{19}Cd_2N_2O_{11.5}$ (M_r = 708.18): C, 35.61; H, 2.70; N, 3.96. Found: C, 35.45; H, 2.90; N, 4.11. IR (cm^{-1}): 3411 (w), 1566 (s), 1377 (m), 1354 (s), 1292 (m), 1014 (w), 834 (w), 745 (s), 430 (w).

Synthesis of $[Cu_2(H_2L)(bpy)_2]$ (7). To 10 mL of an ethanol−water [1:4 (v/v)] solution was added $Cu(CH_3COO)_2\cdot H_2O$ (40.0 mg, 0.20 mmol), bpy (31.2 mg, 0.20 mmol), and H_4L (25.4 mg, 0.10 mmol) with stirring at room temperature. After a few minutes, the cloudy solution was sealed in a Teflon reactor (15 mL), which was heated at 140 °C for 3 days and then cooled to room temperature at 10 °C·h^{-1}. The initial pH value for **7** was 4.0. Blue crystals of **7** were collected in 60% yield [based on $Cu(CH_3COO)_2$]. ICP analysis of **7** gave the content of Cu as 13.62% (calcd 13.47%). Anal. Calcd for $C_{40}H_{24}Cu_2N_4O_{16}$ (M_r = 943.71): C, 50.91; H, 2.56; N, 5.93. Found: C, 50.82; H, 2.43; N, 6.09. IR (cm^{-1}): 3168 (w), 1627 (m), 1573 (m), 1347 (s), 1292 (m), 1112 (m), 885 (w), 784 (s), 669 (w), 425 (w).

Synthesis of $[Cu_2(L)(bpy)(H_2O)]$ (8). The preparation of **8** was similar to that of **7** except that a Na_2CO_3 solution (0.2 mol·L^{-1}) was used to adjust the pH value to 5.2. Green and blue crystals were obtained. The blue ones were not good enough for X-ray diffraction analysis, and the green ones were collected in 34% yield [based on $Cu(CH_3COO)_2$]. ICP analysis of **8** gave the content of Cu as 23.32% (calcd 23.05%). Anal. Calcd for $C_{20}H_{12}Cu_2N_2O_9$ (M_r = 551.41): C, 43.56; H, 2.20; N, 5.08. Found: C, 43.44; H, 2.01; N, 4.89. IR (cm^{-1}): 3448 (w), 3120 (w), 1523 (m), 1115 (m), 942 (s), 908 (s), 837 (s), 709 (m), 654 (m), 449 (w).

Synthesis of $[Cu_2(L)(bpy)_{1.5}(H_2O)_{2.5}]$ (9). The preparation of **9** was similar to that of **8** except that the temperature was 130 °C instead of 140 °C. Blue crystals of **9** were collected in 50% yield [based on $Cu(CH_3COO)_2$]. ICP analysis of **9** gave the content of Cu as 19.21% (calcd 19.36%). Anal. Calcd for $C_{25}H_{19}Cu_2N_3O_{10.5}$ (**9**) (M_r = 656.51): C, 45.73; H, 2.92; N, 6.40. Found: C, 45.62; H, 3.09; N, 6.31. IR (cm^{-1}): 3430 (w), 3019 (w), 1541 (m), 1107 (m), 939 (s), 914 (s), 835 (s), 720 (s), 648 (m), 435 (w).

X-ray Crystallography. Single-crystal X-ray diffraction data for compounds **1**−**3**, **5**, **8**, and **9** were recorded on an Oxford Diffraction Gemini R Ultra diffractometer with graphite-monochromated Mo Kα radiation (λ = 0.710 73 Å) at 293 K. Crystallographic (diffraction) data for compounds **4**, **6**, and **7** were collected on a Rigaku RAXIS-RAPID single-crystal diffractometer with Mo Kα radiation (λ = 0.710 73 Å) at 293 K. Absorption corrections were applied using a multiscan technique. All of the structures were solved by the direct methods of *SHELXS-97*[14] and refined by full-matrix least-squares techniques using the *SHELXL-97* program.[15] The H atoms attached to C atoms were generated geometrically. Some aqua and solvent H atoms of compounds **1**, **4**, and **6** were not included in the model. Other H atoms of water molecules and carboxyl H atoms were located from difference Fourier maps and refined with isotropic displacement parameters. Non-H atoms of complexes **2**, **3**, **5**, **7**, and **9** were refined with anisotropic temperature parameters. Some C and O atoms of complexes **1**, **4**, **6**, and **8** were refined with isotropic temperature parameters. The disordered O atoms of compound **4** (O2W, O4W, and O5W), the disordered C and O atoms of compound **6** (C22 and O9), and the disordered C atoms of compound **8** (C16 and C17) were refined using C atoms split over two sites. The H atoms of the disordered C and O atoms were not included in the model. To refine the structure with a reasonable mode, the C−C, C−O, O−O, O−H, and H···H distances of **1**−**6**, **8**, and **9** were restrained to a reasonable range, respectively. The maximum residual electron density is 1.89 e·Å^{-3} at 1.2 Å from O2W for compound **4**, 1.09 e·Å^{-3} at 0.4 Å from O5W for compound **6**, 1.37 e·Å^{-3} at 1.0 Å from C32 for compound **7**, and 1.38 e·Å^{-3} at 2.0 Å from Cu2 for compound **8**.

The detailed crystallographic data and structure refinement parameters for **1**−**9** are summarized in Table 1. Selected bond distances and angles for compounds **1**−**9** are listed in Tables S1−S9 in the Supporting Information.

Results and Discussion

Syntheses. Among the coordination polymers **1**−**9**, compounds **1**−**4** contain L anions, while **5**−**9** consist of both L anions and secondary N-donor ligands (biim-4 or bpy ligands). The reactions of H_4L acid and $M(CH_3COO)_2$ (M = Mn, Cd, Zn, and Cu) only gave crystals of **1**−**4**, while other reactions produced a powder solid. When biim-4 was employed as a secondary N-donor ligand to react with H_4L acid and $M(CH_3COO)_2$ (M = Mn, Cd, Zn, and Cu), only compound **5** was crystallized. Other experiments gave powder forms or very small polycrystals, which were not good enough for X-ray diffraction analysis. However, when the bpy ligand was used as a secondary N-donor ligand in the reaction of H_4L acid and $M(CH_3COO)_2$ (M = Mn, Cd, Zn, and Cu), compounds **1**, **3**, **4**, and **6**−**9** were produced. As we mentioned above, compounds **6**−**9** are composed of L anions and bpy ligands, whereas compounds **1**, **3**, and **4** are only completed by L anions. It is clear that the bpy ligands are not introduced into the structures of **1**, **3**, and **4**, which may be caused by the structural stabilization of the three compounds. The result indicates that compounds **1**, **3**, and **4** can be synthesized not only by the reactions of H_4L acid and $M(CH_3COO)_2$ (M = Mn and Zn) but also by the reactions of H_4L acid, bpy

(14) Sheldrick, G. M. *SHELXS-97, Programs for X-ray Crystal Structure Solution*; University of Göttingen: Göttingen, Germany, 1997.
(15) Sheldrick, G. M. *SHELXL-97, Programs for X-ray Crystal Structure Refinement*; University of Göttingen: Göttingen, Germany, 1997.

Table 1. Crystal Data and Structure Refinements for Compounds **1**−**9**

	1	**2**	**3**	**4**
formula	$C_{10}H_{12}Mn_2O_{13}$	$C_5H_3CdO_5$	$C_{20}H_{16}O_{24}Zn_5$	$C_{20}H_{18}Zn_5O_{25}$
fw	450.08	255.47	967.18	985.20
cryst syst	monoclinic	monoclinic	monoclinic	orthorhombic
space group	$P2_1/c$	$C2/c$	$P2_1/c$	$Pnna$
a (Å)	12.032(6)	15.674(7)	7.2270(18)	15.987(2)
b (Å)	6.574(3)	10.578(4)	15.907(3)	12.056(3)
c (Å)	18.471(8)	7.433(4)	11.981(3)	15.383(3)
α (deg)	90	90	90	90
β (deg)	105.201(5)	110.763(6)	106.874(3)	90
γ (deg)	90	90	90	90
V (Å^3)	1409.9(11)	1152.4(9)	1318.0(5)	2964.9(9)
Z	4	8	4	8
D_{calcd} [g·cm^{-3}]	1.868	2.945	2.437	2.207
F(000)	904	968	956	1952
obsd/unique reflections	8869/3344	3913/1388	8794/3180	14 023/2615
R(int)	0.0370	0.0405	0.0403	0.1128
GOF on F^2	1.087	0.893	0.915	0.934
R1[a] [$I > 2\sigma(I)$]	0.1085	0.0230	0.0303	0.0683
wR2[b] [$I > 2\sigma(I)$]	0.3159	0.0390	0.0605	0.1794

	5	**6**	**7**
formula	$C_{15}H_{17}Zn_2N_2O_{12}$	$C_{21}H_{19}Cd_2N_2O_{11.5}$	$C_{40}H_{24}Cu_2N_4O_{16}$
fw	548.05	708.18	943.71
cryst syst	triclinic	monoclinic	monoclinic
space group	$P\bar{1}$	$C2/c$	$P2_1/c$
a (Å)	8.911(6)	11.941(5)	16.382(4)
b (Å)	10.240(7)	28.171(10)	17.179(4)
c (Å)	12.241(7)	17.316(8)	13.067(5)
α (deg)	73.252(5)	90	90
β (deg)	71.644(6)	103.634(16)	101.812(11)
γ (deg)	64.380(7)	90	90
V (Å^3)	940.7(11)	5661(4)	3599.5(18)
Z	2	8	4
D_{calcd} [g·cm^{-3}]	1.935	1.662	1.741
F(000)	554	2776	1912
obsd/unique reflections	7417/4336	27 069/6470	34 215/8195
R(int)	0.0531	0.0790	0.0745
GOF on F^2	0.762	1.011	1.039
R1[a] [$I > 2\sigma(I)$]	0.0401	0.0579	0.0531
wR2[b] [$I > 2\sigma(I)$]	0.0526	0.1476	0.1207

	8	**9**
formula	$C_{20}H_{12}Cu_2N_2O_9$	$C_{25}H_{19}Cu_2N_3O_{10.5}$
fw	551.41	656.51
cryst syst	monoclinic	monoclinic
space group	$P2_1/n$	$C2$
a (Å)	9.898(5)	21.2840(13)
b (Å)	18.431(8)	11.133(3)
c (Å)	10.993(6)	11.031(6)
α (deg)	90	90
β (deg)	103.378(5)	117.343(7)
γ (deg)	90	90
V (Å^3)	1951.0(17)	2321.8(14)
Z	4	4
D_{calcd} [g·cm^{-3}]	1.877	1.878
F(000)	1104	1328
obsd/unique reflections	9892/4249	12 539/5430
R(int)	0.0728	0.0432
GOF on F^2	0.876	0.899
R1[a] [$I > 2\sigma(I)$]	0.0572	0.0346
wR2[b] [$I > 2\sigma(I)$]	0.1217	0.0554

[a] $R1 = \sum||F_o| - |F_c||/\sum|F_o|$. [b] $wR2 = |\sum w(|F_o|^2 - |F_c|^2)|/\sum|w(F_o^2)^2|^{1/2}$.

ligand, and $M(CH_3COO)_2$ (M = Mn and Zn). Nevertheless, the yield of the former is much higher than that of the latter. In order to investigate the coordination modes of the L anions and the topologies of the resulting frameworks, we carried out numerous parallel experiments by adjusting the pH values from 3.2 to 5.8, changing the reaction temperatures from 130 to 170 °C, and varying the ratio of ethanol and water. However, only crystals of compounds **1**−**9** were obtained.

Structure Description of 1. A single-crystal X-ray diffraction study of **1** reveals an infinite 3D coordination polymer that crystallizes in space group $P2_1/c$. The asymmetric unit contains two Mn^{II} atoms, one L anion, and five water molecules (Figure 1a). Both Mn1 and Mn2 ions

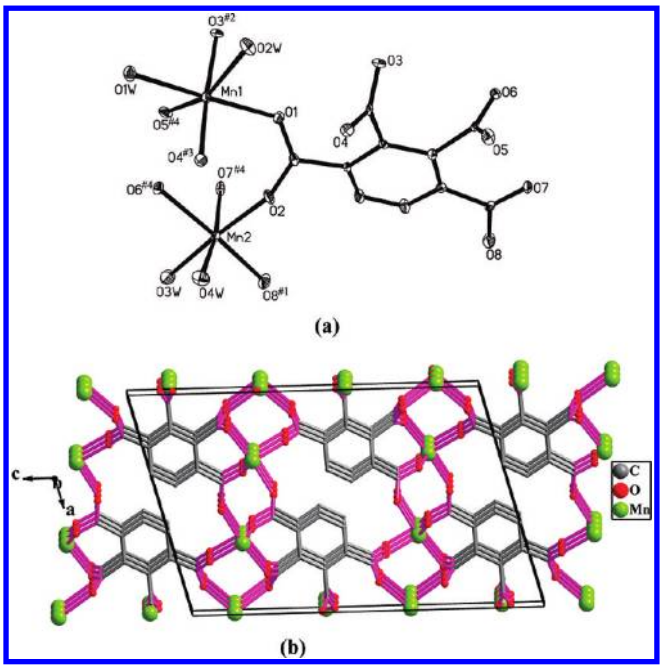

Figure 1. (a) Coordination environment of the Mn^{II} ions in **1** with the solvent water molecule omitted for clarity (30% probability displacement ellipsoids). Symmetry code: #1 = $-x+1, -y+2, -z+1$; #2 = $-x, -y+1, -z+1$; #3 = $-x, -y+2, -z+1$; #4 = $x, -y+1.5, z+0.5$. (b) 3D framework of **1**.

adopt slightly distorted octahedral coordination geometries. The Mn1 ion is six-coordinated by four O atoms from four L anions [Mn1−O1 = 2.170(3) Å, Mn1−$O3^{\#2}$ = 2.276(2) Å, Mn1−$O4^{\#3}$ = 2.196(3) Å, and Mn1−$O5^{\#4}$ = 2.281(3) Å] and two water O atoms [Mn1−O1W = 2.165(3) Å, and Mn1−O2W = 2.223(3) Å] with O5 and O2W atoms located at the apical position. Mn2 is also six-coordinated by four O atoms from three L anions [Mn2−O2 = 2.112(2) Å, Mn2−$O6^{\#4}$ = 2.172(2) Å, Mn2−$O7^{\#4}$ = 2.233(3) Å, and Mn2−$O8^{\#1}$ = 2.121(3) Å] and two water O atoms [Mn2−O3W = 2.180(3) Å, and Mn2−O4W = 2.164(3) Å], with $O1^{\#4}$ and $O7^{\#3}$ atoms occupying the apical position. As shown in Figure S1 in the Supporting Information, each carboxylate group of the L anion bridges two Mn^{II} ions in a bidentate bridging mode. In this mode, two L anions in one unit cell, arranging oppositely in pairs, link the Mn^{II} ions to form a 3D complicated framework of **1** (Figure 1b).

Actually, in order to simplify the rather intricate structure of compound **1**, the L anion can be considered as one 7-connected node. Thus, Mn1 can be reduced to a 4-connected node, and Mn2 can be defined as a 3-connected node. From a topological perspective, the 3D complicated framework of **1** can be described as a rare trinodal (3,4,7)-connected net with a Schläfli symbol of $(4^2\cdot6)(4^5\cdot6)(4^7\cdot6^8\cdot8^6)$ for (Mn2)(Mn1)(L) (Figure S2 in the Supporting Information). Topologies with uninodal and binodal connections, such as 4- and (3,4)-connected nets, are abundant.[16] Nonetheless, only a limited number of trinodal toplogical nets have been given so far.[17] To the best of our knowledge, this is the first example of a (3,4,7)-connected net of a MOF based on carboxylates.[17a]

In addition, there are intermolecular hydrogen-bonding interactions between the water molecules and the carboxylate O atoms. The existence of the hydrogen bonds further stabilizes the structure of the 3D framework.

Structure Description of 2. When the Mn^{II} ion was replaced by a Cd^{II} ion under the similar synthetic conditions, a α-Po net of **2** was obtained. As shown in Figure 2a, the structure of **2** contains one Cd^{II} ion, half of an L anion, and one coordinated water molecule. The Cd^{II} ion is seven-coordinated by six O atoms from four L anions [Cd1−O1 = 2.575(3) Å, Cd1−$O1^{\#1}$ = 2.301(3) Å, Cd1−O2 = 2.298(2) Å, Cd1−$O2^{\#3}$ = 2.664(3) Å, Cd1−$O3^{\#2}$ = 2.279(2) Å, and Cd1−$O4^{\#3}$ = 2.271(2) Å] and one O atom from one water molecule [Cd1−O1W = 2.259(3) Å] in a pentagonal-bipyramidal coordination geometry with O1W and $O1^{\#1}$ atoms located at the apical position. As illustrated in Figure S3 in the Supporting Information, each L anion coordinates to eight Cd^{II} ions with its four carboxylate groups. The carboxylate groups in the 1 and 4 positions show tetradentate bridging modes (μ_4-η^2:η^2), while those in the 2 and 3 positions exhibit bidentate bridging modes. The carboxylate O3 and O4 and their symmetry-related atoms link the Cd^{II} ions to generate a 2D Cd−O layer in the *bc* plane, in which six carboxylate O atoms bridge six Cd^{II} ions to form a 12-membered ring (Figure 2b). The adjacent 2D Cd−O layers are further pillared by the L anions to furnish a complex 3D framework (Figure 2b).

The symmetry-related O3 atoms of two L anions bridge the two adjacent Cd^{II} atoms to generate a $[Cd_2O_2]$ dimer unit (Figure 2b). As shown in Figure S4 in the Supporting Information, if the $[Cd_2O_2]$ dimer unit and the carboxylate groups connected to the unit can be considered as one connecting node, the overall topology of the 3D framework can be regarded as α-Po net.

Structure Description of 3. When the Zn^{II} ion was utilized in place of the Mn^{II} ion of **1** under similar synthetic conditions, a binodal (4,8)-connected net was formed in the structure of **3**. As shown in Figure 3a, the structure of **3** contains two and a half Zn^{II} ions, one L anion, and three water molecules. There are three types of coordination environments around the Zn^{II} ions in the crystal structure. Zn1, which is at the center of a slightly distorted octahedral coordination geometry, is six-coordinated by four carboxylate O atoms [Zn1−O3 = 2.076(2) Å, and Zn1−O7 = 2.1300(19) Å] and two water O atoms [Zn1−O1W = 2.133(2) Å]. Zn2 is surrounded by five carboxylate O atoms [Zn2−$O2^{\#2}$ = 2.137(2) Å, Zn2−O4 = 1.987(2) Å, Zn2−$O6^{\#3}$ = 2.114(2) Å, Zn2−$O7^{\#1}$ = 2.078(2) Å, and Zn2−$O8^{\#3}$ = 2.194(2) Å] and one water O atom [Zn2−O2W = 2.082(2) Å], in a slightly distorted octahedral coordination geometry. However, the Zn3

(16) (a) Gardner, G. B.; Venkataraman, D.; Moore, J. S.; Lee, S. *Nature* **1995**, *374*, 792. (b) Reineke, T. M.; Eddaoudi, M.; O'Keeffe, M.; Yaghi, O. M. *Angew. Chem., Int. Ed.* **1999**, *38*, 2590. (c) Carlucci, L.; Ciani, G.; Proserpio, D. M.; Sironi, A. *J. Am. Chem. Soc.* **1995**, *117*, 4562. (d) Carlucci, L.; Ciani, G.; Proserpio, D. M.; Sironi, A. *Angew. Chem., Int. Ed. Engl.* **1996**, *35*, 1088. (e) Blatov, V. A.; Carlucci, L.; Ciani, G.; Proserpio, D. M. *CrystEngComm* **2004**, *6*, 377. (f) Dong, Y.-B.; Jiang, Y.-Y.; Li, J.; Ma, J.-P.; Liu, F.-L.; Tang, B.; Huang, R.-Q.; Batten, S. R. *J. Am. Chem. Soc.* **2007**, *129*, 4520.

(17) (a) Zhan, S.-Z.; Li, M.; Hou, J.-Z.; Ni, J.; Li, D.; Huang, X.-C. *Chem.—Eur. J.* **2008**, *14*, 8916. (b) Xue, M.; Zhu, G.; Ding, H.; Wu, L.; Zhao, X.; Jin, Z.; Qiu, S. *Cryst. Growth Des.* **2009**, *9*, 1481. (c) Ren, P.; Chen, P.-K.; Xu, G.-F.; Chen, Z. *Inorg. Chem. Commun.* **2007**, *10*, 836.

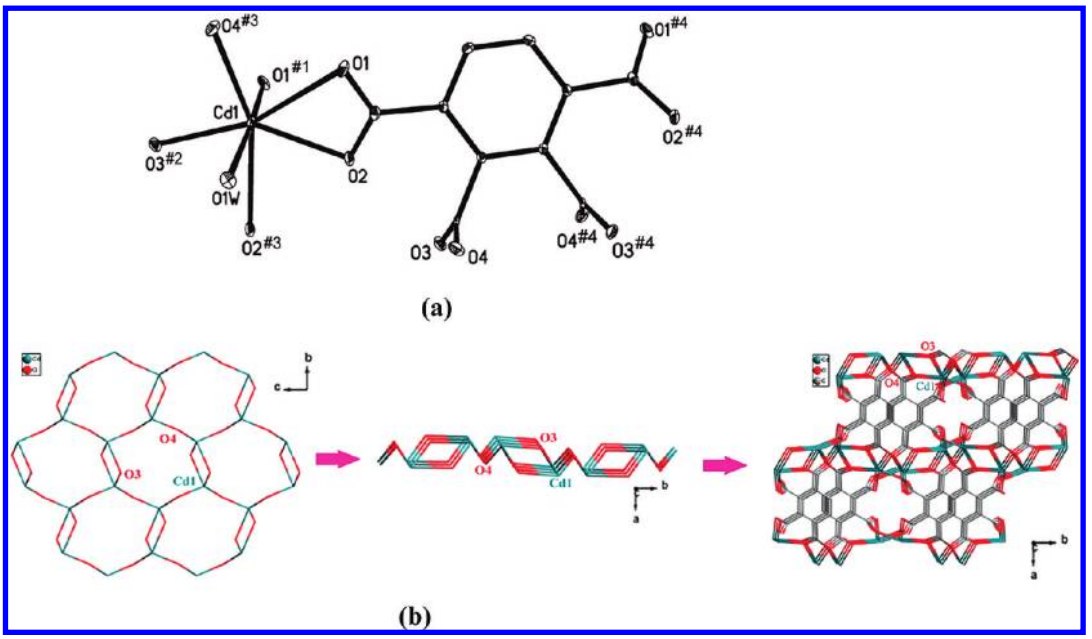

Figure 2. (a) Coordination environment of the Cd^{II} ion in **1** (30% probability displacement ellipsoids). Symmetry code: #1 = ^{x}, $-^{y}$, $^{z}-{}^{1}/_{2}$; #2 = $1-x$, $-y+{}^{1}/_{2}$, $-z$; #3 = $-x+1$, $y-{}^{1}/_{2}$, $-z+{}^{1}/_{2}$; #4 = $-x+1$, y, $-z+{}^{1}/_{2}$. (b) Representation of the 3D framework composed of 2D Cd−O layers and L anions, viewed along the *c* axis.

ion is five-coordinated by five carboxylate O atoms [Zn3−O1 = 2.022(2) Å, Zn3−$O5^{\#4}$ = 2.047(2) Å, Zn3−$O6^{\#4}$ = 2.452(2) Å, Zn3−O7 = 1.986(2) Å, and Zn3−$O9^{\#5}$ = 1.935(2) Å], in a distorted square-pyramidal geometry. As shown in Figure S5 in the Supporting Information, each L anion connects to seven Zn^{II} ions with its four carboxylate groups. Three of the carboxylate groups exhibit bidentate bridging modes, while the fourth adopts a tridentate (μ_3-η^1:η^2) mode. As shown in Figure 3b, one Zn1 ion, two symmetry-related Zn2 ions, and two symmetry-related Zn3 ions are connected by two carboxylate groups and two μ_3-O atoms to furnish a pentanuclear cluster. In this cluster, Zn2 and Zn1 ions are bridged by one carboxylate group and one μ_3-O7 atom, while Zn3 and Zn1 ions are only linked by one μ_3-O7 atom. Further, the pentanuclear clusters are bridged by eight L anions to generate a 3D framework (Figures 3c and S6 in the Supporting Information).

Better insight into such an intricate framework can be accessed by reducing multidimensional structures to simple node-and-connecting nets. Each L anion connects to four pentanuclear clusters, and each pentanuclear cluster is linked by eight L anions. So, the L anion can be assigned to a 4-connected node, and the pentanuclear cluster can be considered as an 8-connected node. Accordingly, the 3D complex framework of **3** can be simplified to a binodal (4,8)-connected topology. As shown in Figure S7 in the Supporting Information, the combination of nodes and connectors provides the unusual (4,8)-connected network of compound **3** with the topological notation of $(4^5\cdot6)_2(4^{10}\cdot6^{14}\cdot8^4)$. To date, a variety of network topologies based on 4-, (3,4)-, and (3,5)-connected nodes have been realized.[16,18] In contrast, topologies of the coordination polymers with higher connection nodes are relatively rare[19] because of the limited coordination numbers of the central metals and the steric hindrance between the coordinated ligands. Until now, only limited (4,8)-connected nets have been reported, and most of them are fluorite topology frameworks.[20] Here we provide a new example of (4,8)-connected topology with a Schläfli symbol of $(4^5\cdot6)_2(4^{10}\cdot6^{14}\cdot8^4)$.

Structure Description of 4. Compared to **3**, compound **4** was obtained only by adjustment of the pH value of the reaction materials to a higher one. Nonetheless, a quite different (4,8)-connected net was formed. As shown in Figure 4a, the asymmetric unit of **4** consists of two and a half Zn^{II} ions, one L anion, one μ_3-O atom, and three and a half water molecules. Both Zn1 and Zn2 ions are six-coordinated by four carboxylate O atoms [Zn1−O2 = 2.160(6) Å, Zn1−$O7^{\#2}$ = 2.059(7) Å, Zn2−$O6^{\#2}$ = 2.356(6) Å, and Zn2−$O8^{\#3}$ = 2.073(6) Å] and two μ_3-O atoms [Zn1−O9 = 2.069(5) Å, and Zn2−O9 = 2.003(5) Å], displaying slightly distorted octahedral coordination geometries. Nevertheless, the Zn3 ion is four-coordinated by three carboxylate O atoms [Zn3−$O1^{\#1}$ = 1.952(7) Å, Zn3−O4 = 2.023(7) Å, and Zn3−$O5^{\#4}$ = 1.969(6) Å] and one μ_3-O atom [Zn3−O9 = 1.964(6) Å], adopting a distorted tetrahedral geometry. The most interesting feature of **4** is that the Zn4 ion is six-coordinated by six water molecules [Zn4−O3W = 2.08(2) Å, Zn4−O4W = 1.90(4) Å, Zn4−O5W = 1.98(5) Å, and Zn4−O6W = 2.118(13) Å] in a slightly distorted octahedral coordination geometry, generating a discrete $[Zn(H_2O)_6]^{2+}$ cation. Each L anion coordinates to seven Zn^{II} ions with its four carboxylate groups. Three carboxylate groups of the L anion display bidentate bridging modes, while the fourth exhibits a monodentate mode (Figure S8 in the Supporting Information). The carboxylate O atoms of the L anions and the μ_3-O atoms bridge five symmetry-related

(18) He, H.; Da, F.; Sun, D. *Dalton Trans.* **2009**, 763.
(19) Li, S.-L.; Lan, Y.-Q.; Qin, J.-S.; Ma, J.-F.; Su, Z.-M. *Cryst. Growth Des.* **2008**, *8*, 2055.
(20) (a) Chun, H.; Kim, D.; Dybtsev, D. N.; Kim, K. *Angew. Chem., Int. Ed.* **2004**, *43*, 971. (b) Dincă, M.; Dailly, A.; Long, J. R. *Chem.—Eur. J.* **2008**, *14*, 10280.

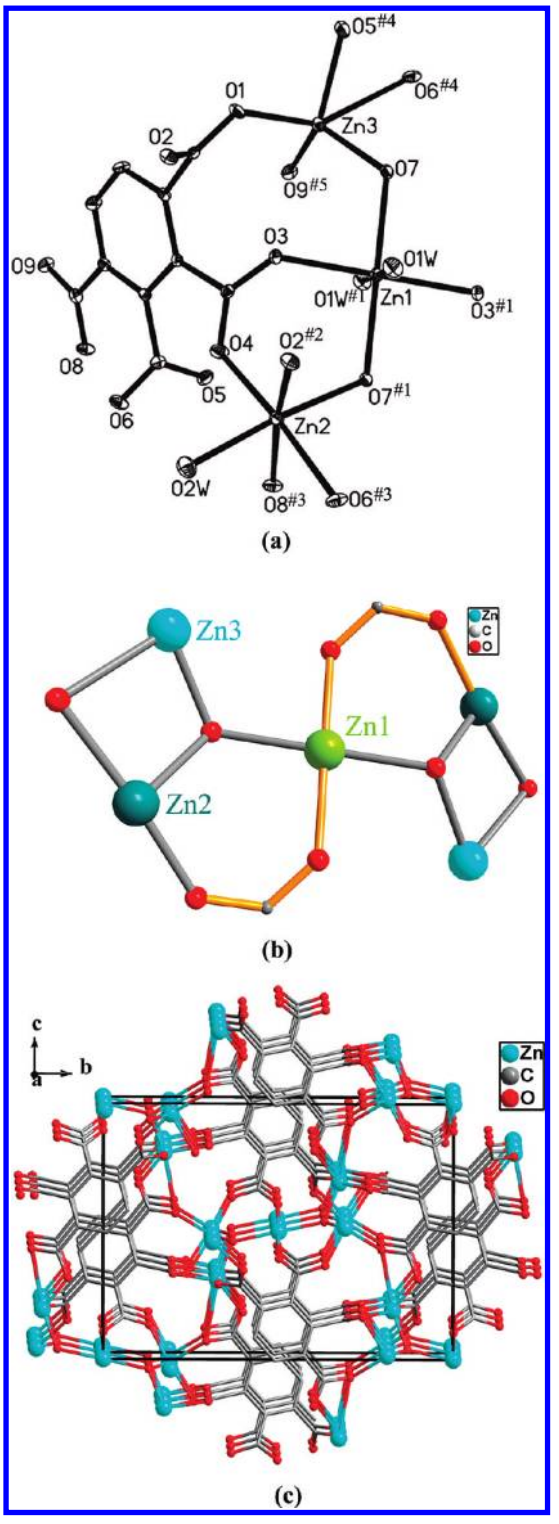

Figure 3. (a) Coordination environment of the Zn^{II} ion in **3** with the solvent water molecules omitted for clarity (30% probability displacement ellipsoids). Symmetry code: #1 = $-x, -y, -z$; #2 = $-x-1, -y, -z$; #3 = $x, -y+{}^1/_2, z-{}^1/_2$; #4 = $-x, y-{}^1/_2, -z+{}^1/_2$; #5 = $-x, -y, -z+1$. (b) Pentanuclear cluster of compound **3**. (c) Representation of the 3D framework of **3**.

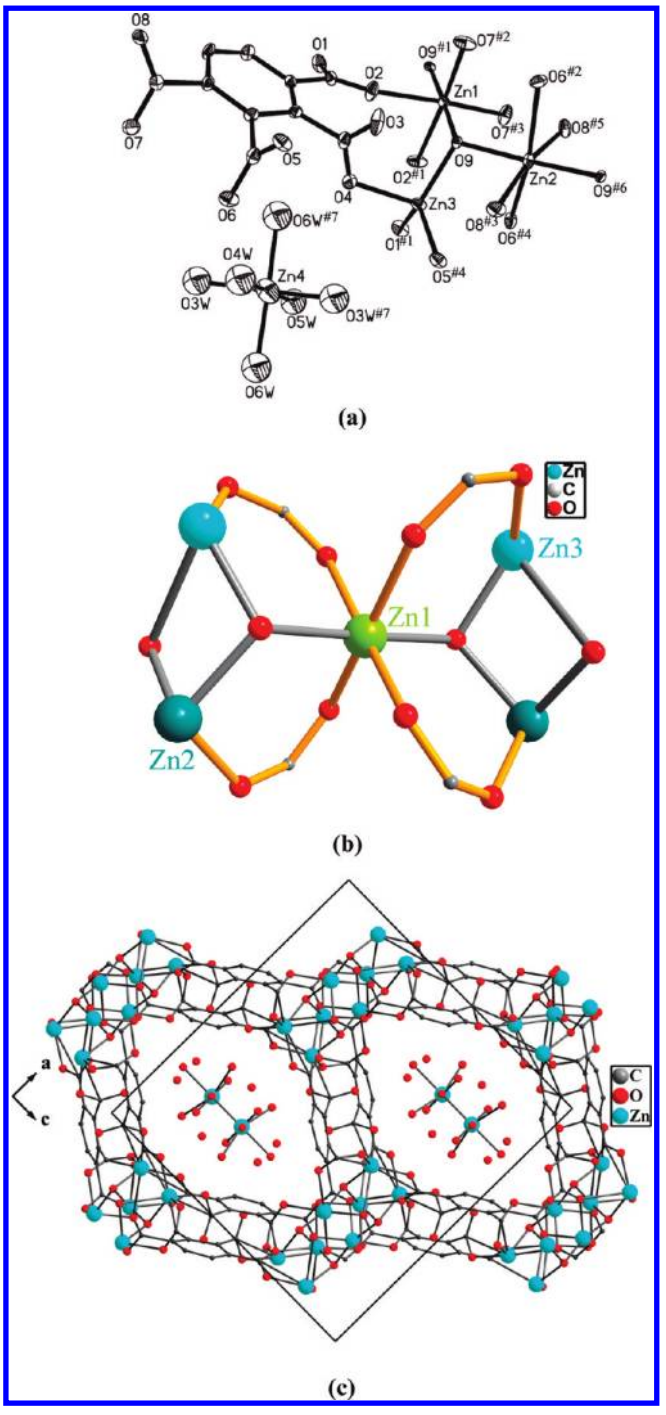

Figure 4. (a) Coordination environment of the Zn^{II} ions in **4** with the solvent water molecules omitted for clarity (30% probability displacement ellipsoids). Symmetry code: #1 = $x, -y-{}^1/_2, -z+{}^1/_2$; #2 = $x-{}^1/_2, y, -z+1$; #3 = $x-{}^1/_2, -y-{}^1/_2, z-{}^1/_2$; #4 = $-x+2, -y, -z+1$; #5 = $-x+2, y+{}^1/_2, z-{}^1/_2$; #6 = $-x+{}^3/_2, -y, z$; #7 = $-x+{}^5/_2, -y, z$. (b) Pentanuclear cluster of compound **4**. (c) Representation of the 3D porous framework of **4** with the $[Zn(H_2O)_6]^{2+}$ cations located in the channels.

Zn^{II} ions to furnish a pentanuclear Zn^{II} cluster (Figure 4b). The pentanuclear cluster is composed of a rectangular arrangement centered on the Zn1 ion. Different from the combination fashion of the cluster in **3**, both Zn2 and Zn3 ions in **4** are bridged by one carboxylate group and one μ_3-O7 atom to the central Zn1 ion, respectively. Another discrepancy is that the two Zn2 ions included in the cluster of **4** are located on one side of the rectangle, whereas the two Zn2 ions contained in the cluster of **3** occupy the diagonal positions of the rectangle. By comparison with the cluster of **3**, a closely constrained pentanuclear Zn^{II} cluster is formed in **4** because of the tighter combination

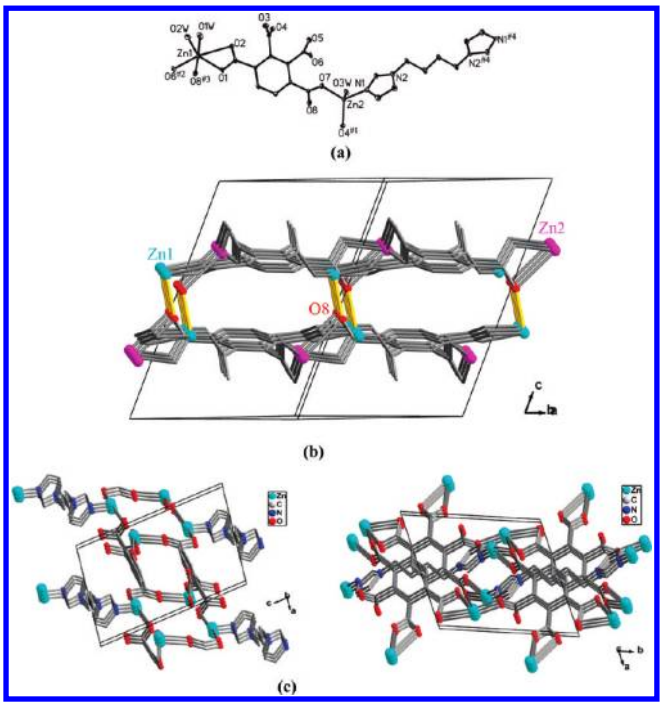

Figure 5. (a) Coordination environment of the Zn^{II} ions in **5** with the solvent water molecule omitted for clarity (30% probability displacement ellipsoids). Symmetry code: #1 = $x+1, y, z$; #2 = $x, y-1, z$; #3 = $-x+1, -y, -z+1$; #4 = $-x+1, -y+2, -z+2$. (b) View of the 2D double layer constructed from Zn^{II} ions and L anions. (c) Representation of the 3D framework of **5** viewed along the *b* (left) and *c* (right) axes.

modes between the Zn ions. Additionally, this can be supported by the Zn···Zn separations [Zn2···Zn2 = 7.203(1) Å for **3** and Zn2···Zn3 = 6.826(2) Å for **4**]. Eight L anions and two μ_3-O atoms are involved in the binding of the tightly arranged pentanuclear Zn^{II} cluster to give a 3D structure (Figures 4c and S9 in the Supporting Information). Interestingly, there are channels of approximately 10.546(3) × 14.713(5) $Å^2$ dimensions viewed along the *b* axis, which are occupied by $[Zn(H_2O)_6]^{2+}$ cations and solvent water molecules. *PLATON*[21] calculations show that the solvent-accessible void is 924.9 $Å^3$ per unit cell volume.

Each pentanuclear cluster of **4** is linked to 12 other ones by 8 L anions. So, from a topological view, if the L anion is considered to be a 4-connected node and the pentanuclear cluster a 8-connected node, respectively, then the framework of **4** becomes a (4,8)-connected net with a Schläfli symbol of $(4^4\cdot6^2)_2(4^{15}\cdot6^{10}\cdot8^3)$ (Figure S10 in the Supporting Information). Despite the fact that the connection nodes and shortest circuits of **4** are the same as those of **3**, their Schläfli symbols are different because of the different coordination modes of the L anions and Zn^{II} ions.

Structure Description of 5. Compared to **3**, when the biim-4 ligand was introduced into **5**, a rare (3,5)-connected net was obtained. As shown in Figure 5a, the asymmetric unit of **5** consists of two Zn^{II} ions, one L anion, half of a biim-4 ligand, and four water molecules. The two Zn^{II} ions show different coordination geometries. Zn1 is six-coordinated by four carboxylate O atoms [Zn1−O1 = 2.031(3) Å, Zn1−O2 = 2.560(2) Å, Zn1−$O6^{\#2}$ = 2.024(3) Å, and Zn1−$O8^{\#3}$ = 2.216(3) Å] and two water O atoms [Zn1−O1W = 2.047(3) Å, and Zn1−O2W = 2.023(3) Å] in a slightly distorted octahedral coordination geometry. Nevertheless, Zn2 is four-coordinated by two carboxylate O atoms [Zn2−$O4^{\#1}$ = 1.958(3) Å, and Zn2−O7 = 1.955(3) Å], one water O atom [Zn2−O3W = 2.020(3) Å], and one N atom from the biim-4 ligand [Zn2−N1 = 1.970(3) Å], exhibiting tetrahedral geometry. Each L anion links five Zn^{II} ions with its four carboxylate groups. The two carboxylate groups in the 2 and 3 positions display monodentate coordination modes, whereas those in the 1 and 4 positions give a bidentate chelate and a bidentate bridging fashion, respectively (Figure S11 in the Supporting Information). If the carboxylate O8 atom is ignored, the L anions connect the Zn^{II} ions to give a 2D layer with four-membered rings (Figure S12 in the Supporting Information). Four L anions, two symmetry-related Zn1 ions, and two symmetry-related Zn2 ions are involved in the construction of the four-membered ring. The adjacent layers are further linked by the symmetry-related O8 atoms to generate a 2D double layer (Figure 5b). The symmetry-related O8 atoms are located between the two layers, whereas other O atoms lie in the layer. As shown in Figure 5c, the biim-4 ligands, adopting a cis conformation, bridge the neighboring double layers to give a 3D framework.

From a topological viewpoint, it is worth noting that the structure of **5** reveals a unique trinodal (3,5)-connected topological net: the six-coordinated Zn1 acts as a 3-connected node [Schläfli symbol $(4^2\cdot6)$]; the four-coordinated Zn2 is also a 3-connected node [Schläfli symbol $(6^2\cdot8)$]; the hexadentate L anion is considered to be a 5-connected node [Schläfli symbol $(4^2\cdot6^2\cdot8^5\cdot10)$]; and the biim-4 ligand is simplified to one linker, respectively. Considering the stoichiometry, the overall topology is (Zn1)(Zn2)(L) with a Schläfli symbol of $(4^2\cdot6)(6^2\cdot8)(4^2\cdot6^2\cdot8^5\cdot10)$ (Figure S13 in the Supporting Information). Up to now, some examples of MOFs containing a binodal (3,5)-connected net have been reported;[18] however, the trinodal (3,5)-connected net has never been observed in the literature.

Structure Description of 6. Compared to **2**, the introduction of a bpy ligand in **6** leads to an uncommon (4,6)-connected topology. As illustrated in Figure 6a, the structure of **6** contains two Cd^{II} ions, one L anion, one bpy ligand, three water molecules, and half of an ethanol molecule. The Cd1 ion is six-coordinated by five O atoms from three L anions [Cd1−O1 = 2.374(5) Å, Cd1−O2 = 2.385(4) Å, Cd1−$O3^{\#1}$ = 2.558(5) Å, Cd1−$O4^{\#1}$ = 2.218(5) Å, and Cd1−$O5^{\#2}$ = 2.236(5) Å] and one N atom from one bpy ligand [Cd1−N1 = 2.281(6) Å] in a highly distorted octahedral geometry, while the Cd2 ion is seven-coordinated by five O atoms from three L anions [Cd2−O2 = 2.349(5) Å, Cd2−$O6^{\#2}$ = 2.308(4) Å, Cd2−$O7^{\#2}$ = 2.386(5) Å, Cd2−$O7^{\#3}$ = 2.432(5) Å, and Cd2−$O8^{\#3}$ = 2.389(5) Å], one O atom from one coordinated water molecule [Cd2−O1W = 2.343(6) Å], and one N atom from one bpy ligand [Cd2−$N2^{\#4}$ = 2.300(6) Å], exhibiting a slightly distorted pentagonal-bipyramidal geometry. Each L anion connects six Cd^{II} ions with its four carboxylate groups. As shown in Figure S14 in the Supporting Information, the carboxylate groups in the

(21) Spek, A. L. *PLATON, A Multipurpose Crystallographic Tool*; Utrecht University: Utrecht, The Netherlands, 2001.

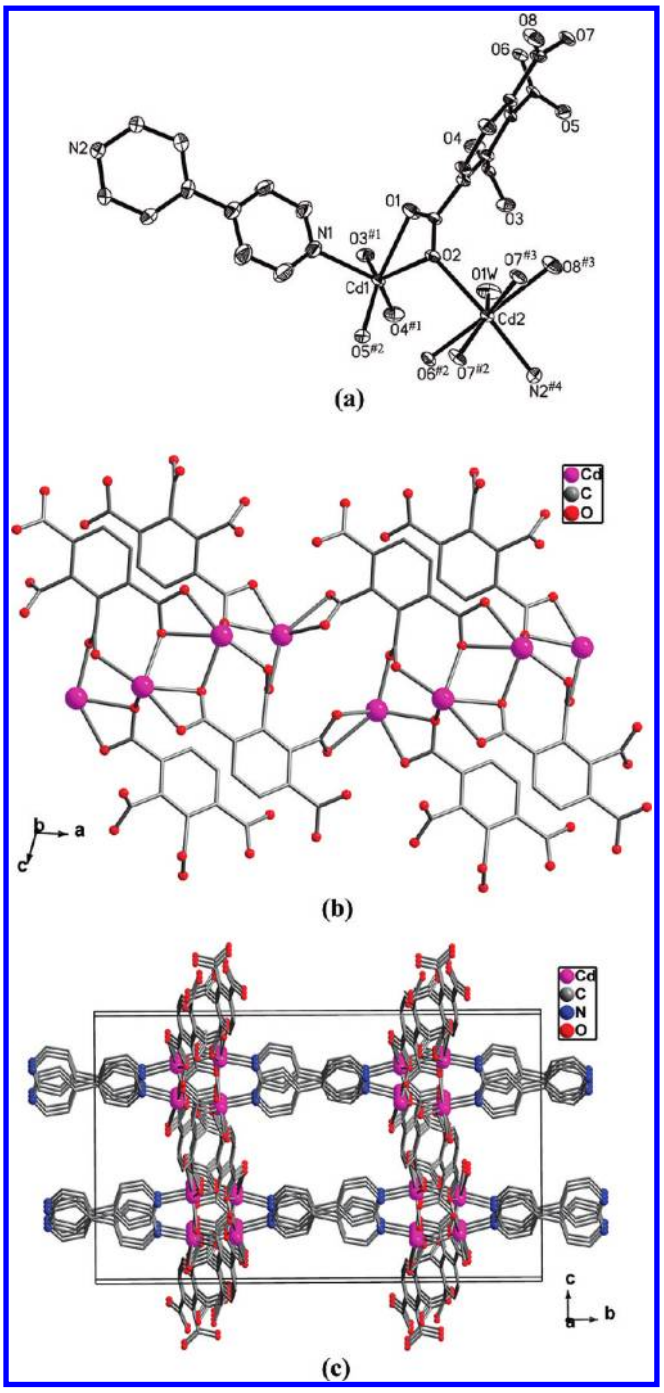

Figure 6. (a) Coordination environment of the Cd^{II} ions in **6** with the solvent water molecules and ethanol molecule omitted for clarity (30% probability displacement ellipsoids). Symmetry code: #1 = $-x + {}^1/_2$, $-y + {}^1/_2$, $-z$; #2 = $x + {}^1/_2$, $-y + {}^1/_2$, $z + {}^1/_2$; #3 = $-x - {}^1/_2$, $-y + {}^1/_2$, $-z$; #4 = $-x + {}^1/_2$, $y + {}^1/_2$, $-z + {}^1/_2$. (b) 2D layer consisting of Cd^{II} ions and L anions. (c) 3D framework of **6**.

1 and 4 positions exhibit tridentate (μ_3-η^1:η^2) coordination modes, while those in the 2 and 3 positions display a bidentate chelate and a bidentate bridging mode, respectively. If the bpy ligand is ignored, the L anion bridges the Cd^{II} ions to generate a 2D neutral layer in the *ac* plane (Figure 6b). In this plane, two adjacent L anions, arranged in opposite positions, act as one unit with the eight carboxylate groups located outside. Each of these units, as well as its neighbors, bridges four symmetry-related Cd^{II} ions to furnish a tetranuclear Cd^{II} cluster using their μ_3-O2 and μ_3-O7 atoms (Figure S15 in the Supporting Information). The bpy ligands further link the 2D neutral layers to form a 3D framework (Figure 6c).

As shown in Figure S16 in the Supporting Information, if the two adjacent L anions are simplified to a 4-connected node and the two bpy ligands (linking to the same tetranuclear cluster) to one linker, the tetranuclear Cd^{II} cluster can be defined as a 6-connected node. Then, the 3D framework can be described as an uncommon (4,6)-connected topology with a Schläfli symbol of $(4^4\cdot6^2)_2(4^4\cdot6^{10}\cdot8)$, which can be defined as a fsc topology according to O'Keeffe.[22] So far, there are only two examples of coordination polymers displaying the fsc topology.[23]

Structure Description of 7. When the Cu^{II} ion was used instead of the Mn^{II} ion in **1**, a rare polythreading framework of **7** was obtained. As illustrated in Figure 7a, the structure of **7** contains two Cu^{II} ions, two H_2L^{2-} anions, and two bpy ligands. Both Cu1 and Cu2 ions are surrounded by four carboxylate O atoms of four L anions [Cu1−O1 = 1.991(3) Å, Cu1−$O8^{\#2}$ = 1.957(3) Å, Cu1−O10 = 1.977(3) Å, Cu1−$O15^{\#1}$ = 1.978(3) Å, Cu2−O2 = 1.971(3) Å, Cu2−$O7^{\#2}$ = 1.971(3) Å, Cu2−O9 = 1.969(3) Å, and Cu2−$O16^{\#1}$ = 1.966(3) Å] and one N atom from one bpy ligand [Cu1−N3 = 2.154(3) Å, and Cu2−N1 = 2.133(4) Å] in square-pyramidal coordination spheres, with the N atoms occupying the apical positions. The H_2L^{2-} anion is partly deprotonated and acts as a tetradentate ligand. The two carboxylate groups in the 1 and 4 positions connect four Cu^{II} ions in bidentate bridging coordination modes (Figure S17 in the Supporting Information). Two neighboring Cu1 and Cu2 ions are joined together through four bidentate bridging carboxylate groups of four H_2L^{2-} anions with Cu···Cu separations of 2.7009(9) Å. As a result, two Cu^{II} ions (Cu1 and Cu2), four H_2L^{2-} anions, and two coordinated bpy ligands constitute a paddle-wheel secondary building unit. As shown in Figure 7b, each paddle-wheel building unit connects four H_2L^{2-} anions, and in turn each H_2L^{2-} anion links two secondary building units to give a 2D layer structure of a 4^4-**sql** net. The 2D layer of **7** has rhombic windows with a side length of 10.918(2) Å and a diagonal measurement of 13.067(5) × 17.197(4) $Å^2$ based on the Cu···Cu distances. The parallel layers are stacked along the *a* axis in an ABAB sequence with an interlamellar distance of ca. 8.603(2) Å. The bpy ligands display a monodentate coordination mode hanging on both sides of the 2D layer as dangling ligands viewed along the *b* axis (Figure S18 in the Supporting Information). Each dangling arm has an effectual length of about 10.515(3) Å, which is longer than the interlamellar distance. As a result, each four-membered rhombic window is threaded by two arms from the above and below layers, thus resulting in a 2D → 3D polythreading motif involving three 2D layers simultaneously (Figure 7c). According to the literature, the polythreading assembled from lower-dimensional motifs with side arms, displaying a 0D → 1D, 0D → 2D, 1D → 2D, or 1D → 3D polythreaded array, is

(22) Dolomanov, O. V.; Blake, A. J.; Champness, N. R.; Schröder, M. *J. Appl. Crystallogr.* **2003**, *36*, 1283.
(23) (a) Lin, J.-D.; Jia, C.-C.; Li, Z.-H.; Du, S.-W. *Inorg. Chem. Commun.* **2009**, *12*, 558. (b) Bi, M.; Li, G.; Hua, J.; Liu, Y.; Liu, X.; Hu, Y.; Shi, Z.; Feng, S. *Cryst. Growth Des.* **2007**, *7*, 2066.

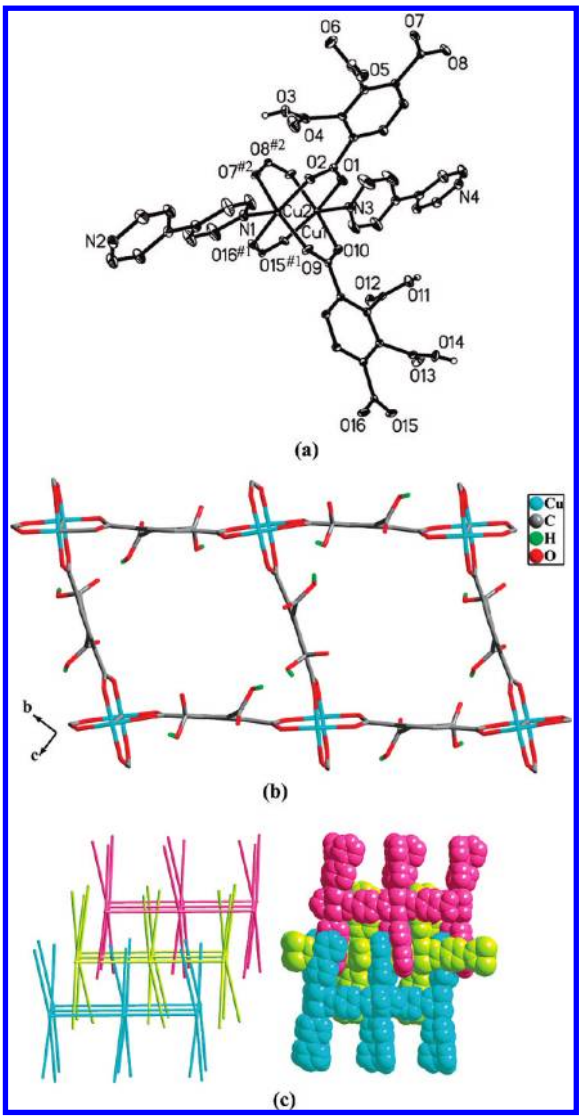

Figure 7. (a) Coordination environment of the Cu^{II} ions in **7** (30% probability displacement ellipsoids). Symmetry code: #1 = $x, -y + {}^1/_2, z - {}^1/_2$; #2 = $x, -y - {}^1/_2, z - {}^1/_2$. (b) 2D layer consisting of paddle-wheel secondary building units. (c) Schematic illustration of the polythreading fashion among three adjacent layers.

common. However, a higher-dimensional motif in this facet is relatively rare.[24]

Notably, classical O−H···N and O−H···O intermolecular hydrogen-bonding interactions are observed among the carboxylate O atoms and bpy N atoms. The intermolecular hydrogen bonds further link the 2D layer structure of **7** to generate a 3D supramolecular framework (Figure S19 in the Supporting Information). It is well-known that the formation of different interpenetrations can be ascribed to the presence of large free voids in a single network.[25] *PLATON*[21] calculations show that the void of this 3D framework of **7** is 583.8 $Å^3$ per unit cell volume, indicating the possibilities of interpenetration of the network. When the hydrogen-bonding interactions are included, the structure of **7** can be defined as a 2-fold-interpenetrated 3D network (Figure 7e).

As shown in Figure S20 in the Supporting Information, if the H_2L^{2-} anion is considered to be a 5-connected node, and the paddle-wheel-like unit a 6-connected node, the hydrogen-bonded 3D framework of **7** can be described as a unique (5,6)-connected 2-fold-interpenetrated network. Each 5-connected H_2L^{2-} anion coordinates to three paddle-wheel-like units, while each paddle-wheel-like unit connects four H_2L^{2-} anions. So, the Schläfli symbol of the (5,6)-connected network can be defined as $(3^2\cdot4\cdot5^2\cdot6^4\cdot7)_4(3^2\cdot4^2\cdot5^4\cdot6^4\cdot7\cdot8^2)_3$. It is worth noting that if the O−H···O intermolecular hydrogen bonds are ignored, the topology of **7** can be described as a rutile net (Figure S21 in the Supporting Information). According to the documents, only one related polythreading rutile net has been reported for the polymer [Zn(HL1)(4,4′-bpy)] (L1 = 1,2,4-benzenetricarboxylate).[24]

Structure Description of 8. When $NaCO_3$ was utilized to adjust the pH value of the reactants of **7**, a trinodal (3,4,5)-connected network of **8** was obtained. As illustrated in Figure 8a, the structure of **8** contains two Cu^{II} ions, one L anion, one bpy ligand, and one water molecule. Both Cu1 and Cu2 ions adopt slightly distorted square-pyramidal geometries. The Cu1 ion is five-coordinated by three O atoms from two L anions [Cu1−O1 = 1.952(4) Å, Cu1−$O3^{\#3}$ = 2.002(4) Å, and Cu1−$O6^{\#3}$ = 1.958(4) Å], one water O atom [Cu1−O1W = 2.365(7) Å], and one N atom from one bpy ligand [Cu1−N1 = 2.009(5) Å], while the Cu2 ion is five-coordinated by four O atoms from three L anions [Cu2−$O4^{\#2}$ = 2.036(4) Å, Cu2−$O5^{\#1}$ = 2.087(4) Å, Cu2−O7 = 2.325(6) Å, and Cu2−O8 = 1.999(12) Å] and one N atom from one bpy ligand [Cu2−N2 = 1.970(5) Å]. Each L anion connects five Cu^{II} ions with its four carboxylate groups. The carboxylate groups in the 2 and 3 positions possess bidentate bridging coordination modes, while those in the 1 and 4 positions show monodentate and bidentate chelate coordination modes, respectively (Figure S22 in the Supporting Information). As illustrated in Figure 8b, if the bpy ligands are ignored, the L anions bridge the Cu^{II} ions to furnish a 3D framework with large open windows. There are two kinds of crystallographically independent bpy ligands coordinated to the Cu^{II} ions and located inside the pores in opposite positions. The Cu···Cu distances across the two kinds of bpy ligands are 11.070(4) Å for Cu1···Cu1 and 10.969(5) Å for Cu2···Cu2, respectively (Figure 8c). Four symmetry-related Cu2 ions, two L anions, and two bpy ligands form a six-membered ring, while three symmetry-related Cu1 ions, two symmetry-related Cu2 ions, four L anions, and one bpy ligand generate a nine-membered ring. The two kinds of ring units interconnect to produce a self-penetrating structural network, in which the bpy ligand, linking the Cu1 ions, penetrates through the six-membered ring (Figures S23 and S24 in the Supporting Information).

From a topological viewpoint, the Cu1 ion can be simplified to a 3-connected node, the Cu2 ion to a 4-connected node, the L anion to a 5-connected node, and the bpy ligand to one linker. As a result, the topology of **8** can be described as a novel trinodal (3,4,5)-connected network, which has a short vertex symbol of $(7\cdot8^2)(4^2\cdot6^2\cdot7^2)(4^2\cdot6\cdot7^3\cdot8^2\cdot9^2)$. Until now, only one

(24) Qin, C.; Wang, X.; Carlucci, L.; Tong, M.; Wang, E.; Hu, C.; Xu, L. *Chem. Commun.* **2004**, 1876.
(25) Li, X.; Cao, R.; Sun, D.; Bi, W.; Yuan, D. *Eur. J. Inorg. Chem.* **2004**, 2228.

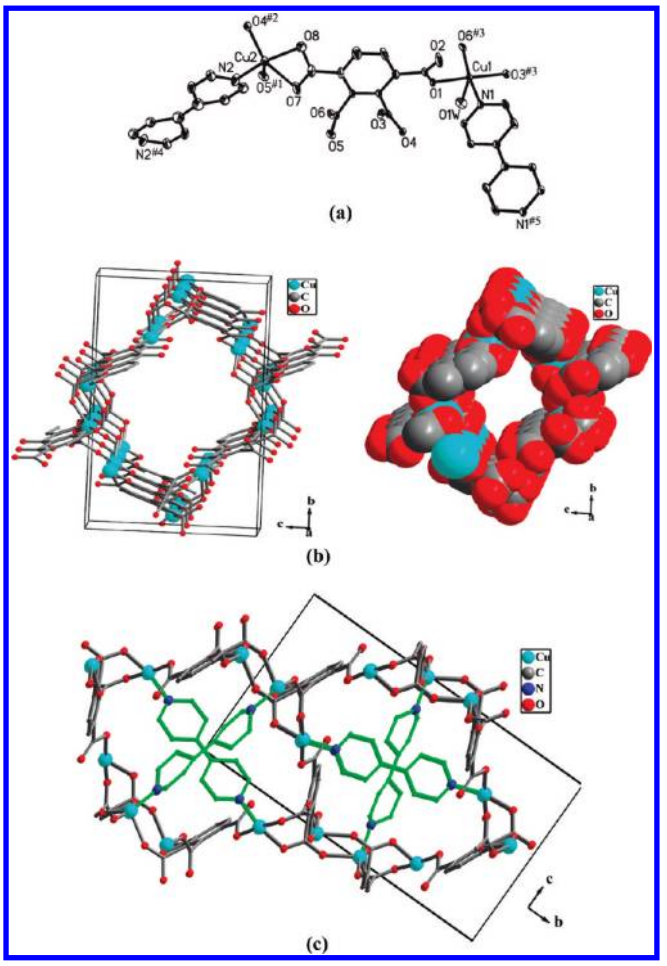

Figure 8. (a) Coordination environment of the Cu^{II} ions in **8** (30% probability displacement ellipsoids). Symmetry code: #1 = $-x-1, -y, -z+1$; #2 = $x-1, y, z$; #3 = $x+{}^1/_2, -y+{}^1/_2, z+{}^1/_2$; #4 = $-x-2, -y, -z$; #5 = $-x+1, -y, -z+2$. (b) 3D porous framework composed of Cu^{II} ions and L anions. (c) View of the 3D structure of **8** with the bpy ligands (green ones) located in the channels across from each other.

example of MOF related to the mixed (3,4,5)-connected topology with a different symbol had been reported.[17b]

Structure Description of 9. Compound **9** was prepared only by changing the reaction temperature of **8** from 140 to 130 °C. In addition, compound **9** is present in each enantiomer in equal amounts. The chiral compound **9** exhibits a unique tetranodal (2,4)-connected net. There are two Cu^{II} ions, one L anion, one and a half bpy ligands, and two and a half water molecules in the unit cell of **9** (Figure 9a). The three Cu^{II} ions display different coordination environments. The Cu1 ion is six-coordinated by two O atoms from two L anions [Cu1−O1 = 2.026(2) Å], two O atoms from two coordinated water molecules [Cu1−O1W = 2.413(3) Å], and two N atoms from two bpy ligands [Cu1−N1 = 2.024(3) Å, and Cu1−$N2^{\#1}$ = 2.021(4) Å] in a slightly distorted octahedral geometry. The Cu2 ion is five-coordinated by four O atoms from two L anions [Cu2−O4 = 1.979(2) Å, and Cu2−O5 = 1.913(2) Å], and one O atom from one coordinated water molecule [Cu2−O2W = 2.245(4) Å], exhibiting a square-pyramidal geometry. The Cu3 ion is four-coordinated by one O atom from one L anion [Cu3−O8 = 1.923(2) Å], one water O atom [Cu3−O3W = 1.964(2) Å], and two N

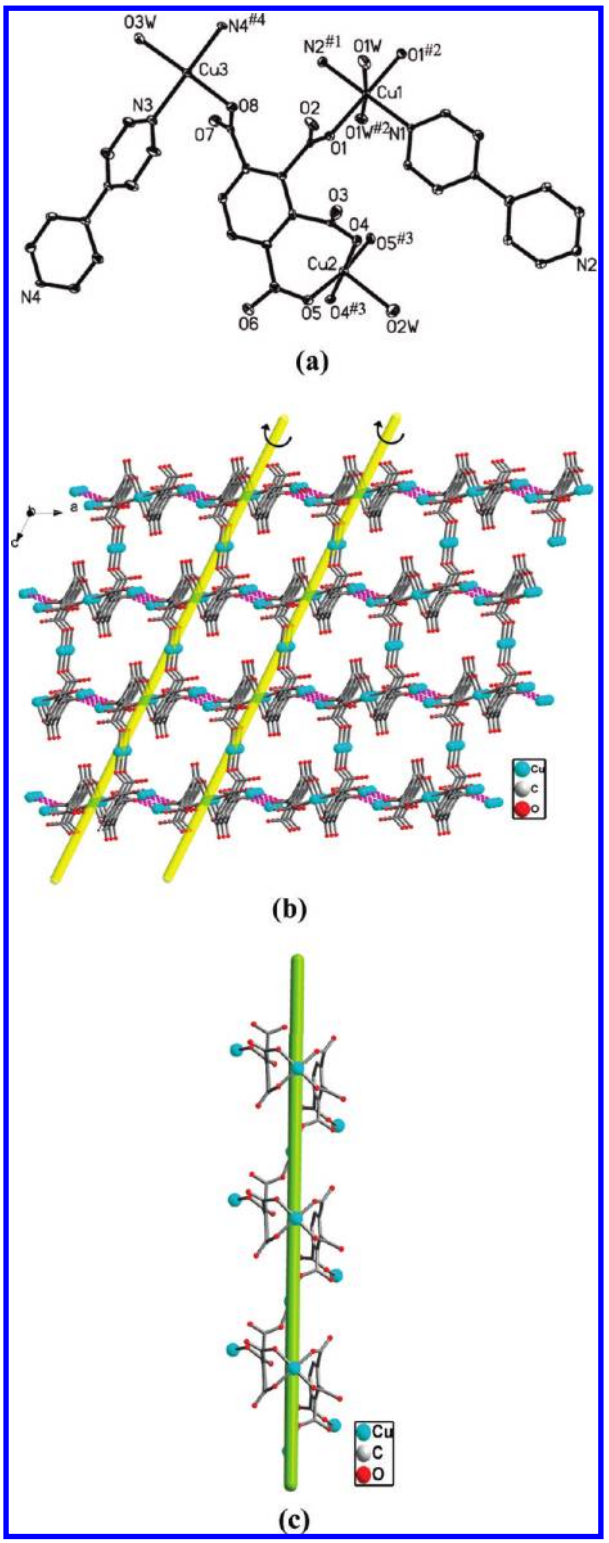

Figure 9. (a) Coordination environment of the Cu^{II} ions in **9** (30% probability displacement ellipsoids). Symmetry code: #1 = $x, y+1, z$; #2 = $-x+1, y, -z+1$; #3 = $-x+1, y, -z+3$; #4 = $x, y, z-1$. (b) View of the 3D chiral structure consisting of L anions and Cu^{II} ions. (c) Left-handed helical chain constructed from Cu^{II} ions and L anions.

atoms of two bpy ligands [Cu3−N3 = 2.007(3) Å, and Cu3−$N4^{\#4}$ = 1.988(3) Å], displaying a distorted square-planar geometry. The four carboxylate groups of L connect three Cu^{II} ions in monodentate coordination modes (Figure S25 in the Supporting Information). As

shown in Figure 9b, given the consideration of the intermolecular contact Cu3···O3 [2.715(3) Å], L anions link the Cu^{II} ions to furnish a chiral 3D Cu−L backbone. It is noteworthy that in the 3D Cu−L backbone of **9** the carboxylates of L bridge the Cu^{II} ions to form a 1D left-handed helical chain running along the *b* axis (Figure 9c). Additionally, there are two kinds of bpy ligands located inside the 3D Cu−L skeletons, which bridge the Cu^{II} ions in vertical directions (Figure S26 in the Supporting Information). The distance between the Cu1 ions across the bpy ligand is 11.133(3) Å along the *b* axis, while that between the Cu3 ions is 11.031(6) Å running along the *c* axis.

As shown in Figure S27 in the Supporting Information, the topology of **9** can be simplified as a tetranodal (2,4)-connected network by considering the Cu1 and Cu3 ions to be 4-connected nodes, the Cu2 ion a 2-connected node, the L ion also a 4-connected node, and the bpy ligand one linker. The short Schläfli topology symbol can be derived by considering the 5-, 6-, 7-, 8-, 10-, and 11-membered rings as the shortest circuits. The 2-connected Cu2 node has a 7-membered shortest circuit; the 4-connected Cu1 node consists of 7- and 11-membered shortest rings, represented by the short Schläfli notation ($7^5\cdot11$); the 4-connected Cu3 node possesses 6-, 7-, and 8-membered shortest circuits, giving the short Schläfli notation of ($6^2\cdot7^3\cdot8$); the 4-connected L node contains 6-, 7-, and 10-membered shortest loops, leading to a Schläfli symbol of ($6\cdot7^4\cdot10$). The molar ratio of these four kinds of connection nodes is Cu2:Cu1:Cu3:L = 1:1:2:2; therefore, the 3D framework of **9** can be described as a tetranodal net displaying a short vertex symbol of $(7)(7^5\cdot11)(6^2\cdot7^3\cdot8)_2(6\cdot7^4\cdot10)_2$. In addition, the 10-membered shortest circuits are passed through by rods of bpy ligands within the single network, leading to a fascinating self-penetrating structure (Figures S27 and S28 in the Supporting Information). Up to now, the tetranodal (2,4)-connected 3D framework has never been observed in MOFs.[26]

Comparison of Structures of 7−9. Although compounds **7**−**9** are all constructed from L anions, Cu^{II} ions, and bpy ligands, they display distinct structures and topologies. The differences of the three compounds are mainly attributed to the different pH values of the reaction system and the different reaction temperatures. **7** displays a 2D → 3D polythreading motif, while **8** gives a 3D self-penetrating framework. In **7**, under a lower pH value, the H_4L acids are partly deprotonated to yield H_2L^{2-} anions, while the bpy ligands are incompletely protonated to form $Hbpy^+$ ions. The H_2L^{2-} anions connect the Cu^{II} ions to furnish a 2D layer structure with the bpy ligands hanging on the two sides of the layer. The 2D layer is threaded by the dangling bpy ligands from the above and below layers, thus resulting in a 2D → 3D polythreading motif. However, in **8**, both the L anions and the bpy ligands are fully deprotonated and link the Cu^{II} ions to give a 3D self-penetrating network. It is clear that the structural differences of the two compounds may be caused by the different pH values of their reaction systems. Compared to the 3D self-penetrating network of **8**, compound **9** exhibits a chiral self-penetrating framework. **9** was prepared at a temperature of 130 °C, while **8** was obtained at a higher temperature (140 °C). The changes of the reaction temperature lead to the different coordination modes of the L anions in compounds **8** and **9** and finally result in the discrepancy of their structures. In **8**, the L anion exhibits bidentate bridging, with monodentate and bidentate chelate coordination modes connecting five Cu^{II} ions, whereas in **9**, the L anion shows monodentate coordination modes linking three Cu^{II} ions. As a result, in **8**, the L anions connect the Cu^{II} ions to give a 3D Cu−L skeleton with 1D channels, while in **9**, the L anions bridge the Cu^{II} ions to generate a 3D chiral Cu−L skeleton. The bpy ligands in **8** and **9** have no contribution to the dimension of the structures but play fundamental roles in the self-penetrating structures. The structural diversity of compounds **7**−**9** indicates that the pH values and reaction temperatures have significant effects on the construction of the frameworks.

Coordination of the L Anion. According to previous studies, many coordination compounds composed of 1,2,4,5-benzenetetracarboxylate anion (L′) have been reported.[27] However, in the compounds based on Mn^{II}, Zn^{II}, Cd^{II}, and Cu^{II} ions, the partly or fully deprotonated L′ anions mainly exhibit monodentate, bidentate bridging, and bidentate chelate coordination modes (Scheme S1 in the Supporting Information).[12b,28,29] The L (or H_2L^{2-}) anions in compounds **1**−**9** display a variety of coordination fashions, connecting to three (compound **9**), four (compound **7**), five (compounds **5** and **8**), six (compound **6**), seven (compounds **1**, **3**, and **4**), or eight (compound **2**) metals. These coordination modes are quite different from those of L′ (or $H_2L'^{2-}$; Scheme S1 in the Supporting Information). Obviously, the different coordination modes between L and L′ anions may be mainly caused by the position discrepancy of the carboxylate groups. In compound **9**, each L anion connects to three Cu^{II} ions in monodentate coordination modes, where those in the 1 and 2 positions coordinate to the same Cu^{II} ion (mode IX, Scheme 2). In this mode, the L anions linked the Cu^{II} ions to furnish left-handed helical chains, which are further linked by the intermolecular contacts (Cu3···O3) and bpy ligands to give a fascinating self-penetrating structure. In **7**, the L anion connects four Cu^{II} ions, where the carboxylate groups in the 1 and 4

(26) Sun, L.-X.; Qi, Y.; Che, Y.-X.; Batten, S. R.; Zheng, J.-M. *Cryst. Growth Des.* **2009**, *9*, 2995.

(27) (a) Sun, D.; Cao, R.; Bi, W.; Weng, J.; Hong, M.; Liang, Y. *Inorg. Chim. Acta* **2004**, *357*, 991. (b) Sun, L.-P.; Niu, S.-Y.; Jin, J.; Yang, G.-D.; Ye, L. *Eur. J. Inorg. Chem.* **2006**, *22*, 5130. (c) Oscar, F.; Jorge, P.; Laura, C.-D.; Fernando, S. D.; Francesc, L.; Miguel, J.; Catalina, R.-P. *Inorg. Chem.* **2008**, *47*, 8053. (d) Oscar, F.; Jorge, P.; Francesc, L.; Miguel, J.; Catalina, R.-P. *CrystEngComm* **2007**, *9*, 815. (e) Kim, J. C.; Alan, J. L.; Kim, H. *Inorg. Chem. Commun.* **2002**, *5*, 771.

(28) (a) Prajapati, R.; Mishra, L.; Kimura, K.; Raghavaiah, P. *Polyhedron* **2009**, *28*, 600. (b) Wu, C.-D.; Lu, C.-Z.; Wu, D.-M.; Zhuang, H.-H.; Huang, J.-S. *Inorg. Chem. Commun.* **2001**, *4*, 561. (c) Song, J.-F.; Zhou, R.-S.; Xu, X.-Y.; Liu, Y.-B.; Wang, T.-G.; Xu, J.-Q. *J. Mol. Struct.* **2008**, *874*, 34. (d) Cao, R.; Shi, Q.; Sun, D.; Hong, M.; Bi, W.; Zhao, Y. *Inorg. Chem.* **2002**, *41*, 6161. (e) Shi, Q.; Cao, R.; Sun, D.-F.; Hong, M.-C.; Liang, Y.-C. *Polyhedron* **2001**, *20*, 3287. (f) Zhao, H.-K.; Ding, B.; Yang, E.-C.; Wang, X.-G.; Zhao, X.-J. *Z. Anorg. Allg. Chem.* **2007**, *633*, 1735.

(29) (a) Diniz, R.; Abreu, H. A. D.; Almeida, W. B. d.; Sansiviero, M. T. C.; Fernandes, N. G. *Eur. J. Inorg. Chem.* **2002**, 1115. (b) Shi, X.; Zhu, G.; Wang, X.; Li, G.; Fang, Q.; Wu, G.; Tian, Ge.; Xue, M.; Zhao, X.; Wang, R.; Qiu, S. *Cryst. Growth Des.* **2005**, *5*, 207. (c) Du, Z.-X.; Li, J.-X.; Zhang, G.-Y.; Hou, H.-W. *Z. Kristallogr. NCS* **2007**, *222*, 107.

Scheme 2. Coordination Modes of the $[H_2L]^{2-}$ and L^{4-} Anions in Compounds **1**−**9**

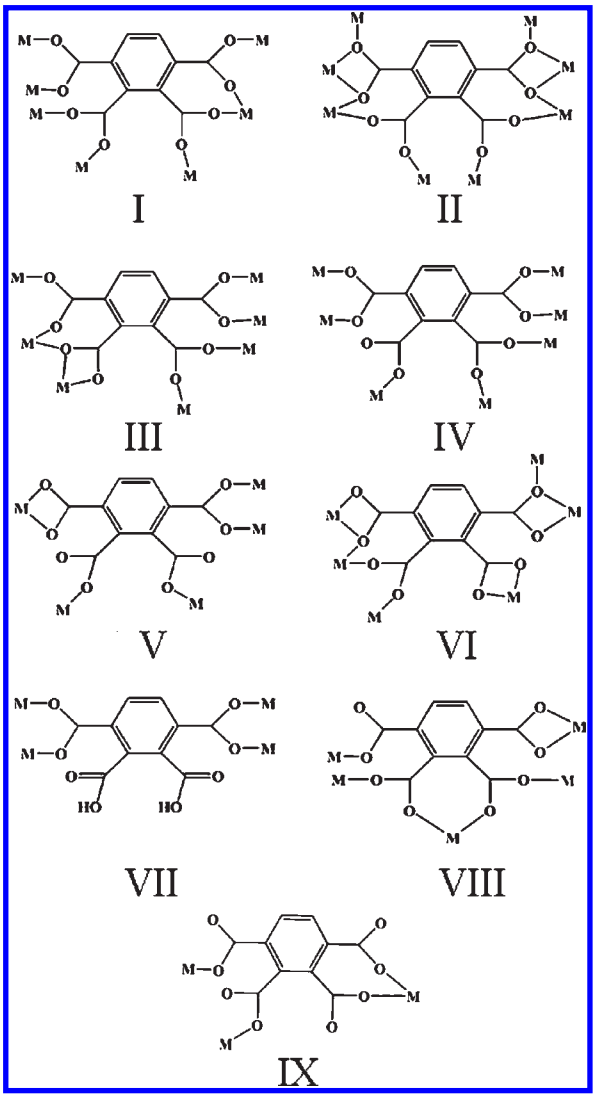

positions of the partly deprotonated H_2L^{2-} anion exhibit the bidentate bridging coordination mode (mode VII, Scheme 2). In this mode, the H_2L^{2-} anions link the Cu^{II} ions to give a 2D layer, which is passed through by the dangling bpy ligands of the neighboring layers to form a rare 2D → 3D polythreading structure. In compounds **5** and **8**, each L anion coordinates to five central metals. However, the coordination fashions of L anions in the two compounds are different. In **5**, the carboxylate groups in the 2 and 3 positions display monodentate coordination modes, while those in the 1 and 4 positions exhibit a bidentate chelate and a bidentate bridging coordination mode, respectively (mode V, Scheme 2). In **8**, the carboxylate groups in the 2 and 3 positions give bidentate bridging coordination modes, while those in the 1 and 4 positions exhibit monodentate and bidentate chelate coordination modes (mode VIII, Scheme 2). As a result, the different coordination modes of the L anions in **5** and **8** lead to the discrepancy of their topologies. In **5**, the L anions link the Zn^{II} ions to provide a 2D double-layer structure, which is further linked by the biim-4 ligands to generate a rare trinodal (3,5)-connected net. However, in **8**, the L anions link the Cu^{II} ions to afford a 3D porous framework, which is further stabilized by bpy ligands. In **6**, each L anion connects six Cd^{II} ions. The carboxylate groups in the 1 and 4 positions show tridentate (μ_3-η^1:η^2) coordination modes, whereas those in the 2 and 3 positions afford bidentate chelate and bidentate bridging coordination modes, respectively (mode VI, Scheme 2). In these modes, the carboxylate groups bridge the Cd^{II} ions to furnish 2D neutral layers, which are further pillared by bpy ligands to form a novel trinodal (3,4,5)-connected network. In **1**, **3**, and **4**, the L anions connect seven central metals. Nevertheless, the coordination fashions of L anions are quite different. In **1**, all four carboxylate groups show bidentate bridging coordination modes, where those in the 1 and 2 positions share the same Mn^{II} ion (mode I, Scheme 2). In these modes, the L anions bridge Mn^{II} ions to form a rare trinodal (3,4,7)-connected network. In **3**, three of the carboxylate groups exhibit bidentate bridging coordination modes, while the fourth displays a tridentate (μ_3-η^1:η^2) coordination mode (mode III, Scheme 2). Two carboxylate groups along with two μ_3-O atoms connect the five symmetry-related Zn^{II} ions to furnish a pentanuclear cluster, which is further bridged by the benzene rings of the L anions to generate a novel binodal (4,8)-connected topology. However, in **4**, three of the carboxylate groups exhibit bidentate bridging coordination modes, while the fourth displays a monodentate coordination mode (mode IV, Scheme 2). Four carboxylate groups and two μ_3-O atoms link five symmetry-related Zn^{II} ions to form a pentanuclear Zn^{II} cluster, which is extended by the benzene rings of the L anions to form a 3D porous framework. In **2**, each L anion bridges eight Cd^{II} ions. The carboxylate groups in the 1 and 4 positions show tetradentate (μ_4-η^2:η^2) coordination modes, whereas those in the 2 and 3 positions display bidentate bridging coordination modes (mode II, Scheme 2). In this mode, the L anions link the $[Cd_2O_2]$ dimer units to furnish a α-Po net. From the above description, we can see that the diversiform coordination fashions of the L anions have a significant effect on the framework structures of the coordination polymers.

Effect of the pH Value and Reaction Temperature on the Framework. The pH value plays a key role in the construction of the frameworks of coordination polymers. The structural differences of **3** and **4**, as well as **7** and **8**, are clearly related to the pH values of the reaction. In most cases, the pH value influences the deprotonation of the organic acids and finally affects the construction of the final product structures. The structural differences of compounds **7** and **8** support this viewpoint. Compound **7** was synthesized under the pH value of 4.0. The partly deprotonated H_2L^{2-} anions connect the Cu^{II} ions to give a 2D 4^4-**sql** net. The linear bpy ligands display monodentate coordination modes and thread the open windows of the adjacent Cu−L layers to give a polythreading framework. When the reaction pH value was adjusted to 5.2, a 3D porous Cu−L backbone of **8** was formed. However, in **8**, the bpy ligands exhibit bidentate coordination modes and further bridge the 3D porous Cu−L backbone. It is clear that a lower pH value of the reaction system can influence the coordination mode of the bpy ligand. Unlike the effect of pH values on the deprotonation of the L anions (**7** and **8**), in **3** and **4**, changes of the pH values can influence the coordination modes of the L

Table 2. Summarized TGA Data of **1**−**9**

	solvent molecule %			residue %			
compound	obsd	calcd	temperature range (°C)	obsd	calcd	temperature (°C)	metallic oxidate
1	19.0	19.99	50−369	35.8	35.07	510	Mn_2O_3
2	8.1	7.05	30−200	48.7	50.26	508	CdO
3	6.6	7.45	50−276	39.7	42.08	552	ZnO
4	13.2	12.97	30−163	40.5	41.20	576	ZnO
5	1.8	3.28	107−134	22.4	29.73	477	ZnO
6	10.5	10.83	30−333	34.8	36.34	521	CdO
7				15.9	16.86	585	CuO
8	3.0	3.16	90−232	27.1	28.86	600	CuO
9	6.4	6.85	49−230	24.9	24.23	580	CuO

anions and the coordination environments of the Zn^{II} ions. Compound **3** was prepared under a pH value of 3.2, while **4** was obtained under a pH value of 4.5. Although in **3** and **4** each L anion connects seven Zn^{II} ions, the coordination modes of the carboxylate groups are different. The carboxylate groups of **3** adopt tridentate (μ_3-η^1:η^2) and bidentate bridging coordination modes. However, the carboxylate groups of **4** display monodentate and bidentate bridging coordination modes. In **3**, the Zn^{II} ions display distorted square-pyramidal and octahedral coordination geometries, which are further linked by the L anions to afford a 3D complex framework. However, in **4**, the Zn^{II} ions possess distorted tetrahedral and octahedral coordination geometries, which are further bridged by the L anions to furnish a 3D porous framework with discrete $[Zn(H_2O)_6]^{2+}$ cations located in the channels.

On the other hand, the reaction temperature also plays a significant role in the construction of the framework structures of coordination polymers. The same reactant ratio, and solvent, but lower synthetic temperatures leads to the transformation of mixed (3,4,5)-connected compound **8** to chiral (2,4)-connected compound **9**. Compound **8** was synthesized under 140 °C. In the resulting structure, the ratio of the bpy ligands to Cu^{II} ions is 1:2. When the reaction temperature was reduced to 130 °C, the ratio of the bpy ligands to Cu^{II} ions in **9** increased to 3:4.

Effect of the Central Metals and Neutral Ligands on the Framework. It should be noted that the central metals also have an important function in the formation of the final structures. Hence, the structural differences of **1**−**3** are mainly caused by changes of the metal ions. The different coordination environments of the central metals are the main reasons for the structural differences in **1**−**3**. In **1**, the two kinds of Mn^{II} ions adopt slightly distorted octahedral coordination geometries. The six-coordinated Mn^{II} ions are connected by the L anions to give a rare trinodal (3,4,7)-connected net. In **2**, the Cd^{II} ion displays a pentagonal-bipyramidal coordination geometry. The seven-coordinated Cd^{II} ions are bridged by the L anions to furnish a α-Po net. In **3**, the two kinds of Zn^{II} ions exhibit slightly distorted octahedral coordination geometries, while the third kind shows a distorted square-pyramidal geometry. The three kinds of unique Zn^{II} ions are linked by the L anions to generate a novel (4,8)-connected net.

The secondary ligands also have a significant effect on the construction of the frameworks. In compounds **3** and **5**, as well as **2** and **6**, the structural differences are primarily affected by the introduction of secondary ligands. Compound **3** is only composed of L anions and Zn^{II} ions, showing a (4,8)-connected network. Nevertheless, when an extra biim-4 ligand is introduced, a structurally different compound **5** was obtained. In **5**, the biim-4 ligands linked the 2D Zn−L double layers to form a 3D trinodal (3,5)-connected net. Compound **2** only consists of the Cd^{II} ions and L anions, affording a α-Po net. Compared to **2**, when the secondary ligand bpy is utilized, a structurally different compound **6** is obtained. In **6**, the linear bpy ligands bridge adjacent 2D Cd−L layers to generate an uncommon (4,6)-connected net.

Thermal Analysis. To characterize the compounds more fully in terms of thermal stability, the thermal behaviors of **1**−**9** were examined by TGA (Figures S29−S37 in the Supporting Information) and the data are summarized in Table 2. The experiments were performed on samples consisting of numerous single crystals under a dinitrogen atmosphere with a heating rate of 10 °C·min^{-1}.

For **1**, the weight loss corresponding to the release of five water molecules is observed from 50 to 369 °C (obsd 19.0%; calcd 19.99%). Decomposition of the residual composition occurred from 400 to 510 °C, leading to the formation of Mn_2O_3 as the residue (obsd 35.8%; calcd 35.07%). From the TGA curve of **2**, the first weight loss occurs from 30 to 200 °C, corresponding to the loss of coordinated water molecule (obsd 8.1%; calcd 7.05%). The removal of the organic components occurred in the range of 200−508 °C. The remaining weight corresponds to the formation of CdO (obsd 48.7%; calcd 50.26%). For **3**, the weight loss, corresponding to the departure of lattice and coordination water molecules, is observed from 50 to 276 °C (obsd 6.6%; calcd 7.45%). The destruction of the remaining compound began from 276 to 552 °C, leading to the formation of ZnO as the residue (obsd 39.7%; calcd 42.08%). For compound **4**, the weight loss in the range of 30−78 °C corresponds to the release of two solvent water molecules (obsd 4.2%; calcd 3.65%) and the removal of the five coordinated water molecules occurred in the temperature range of 78−163 °C (obsd 9.0%; calcd 9.14%). The residual components decomposed from 367 to 576 °C. The remaining residue is of 40.5% corresponding to the formation of ZnO (calcd 41.2%). In comparison with **3**, the stability of the whole structure of **4** is enhanced, which may be caused by the more tightly connected pentanuclear Zn^{II} clusters. The hydrous compound **5** lost its lattice water molecule (obsd 1.8%; calcd 3.28%) from 107 to 134 °C, and then the network decomposed quickly from 335 to 477 °C, leading to the formation of ZnO as the residue

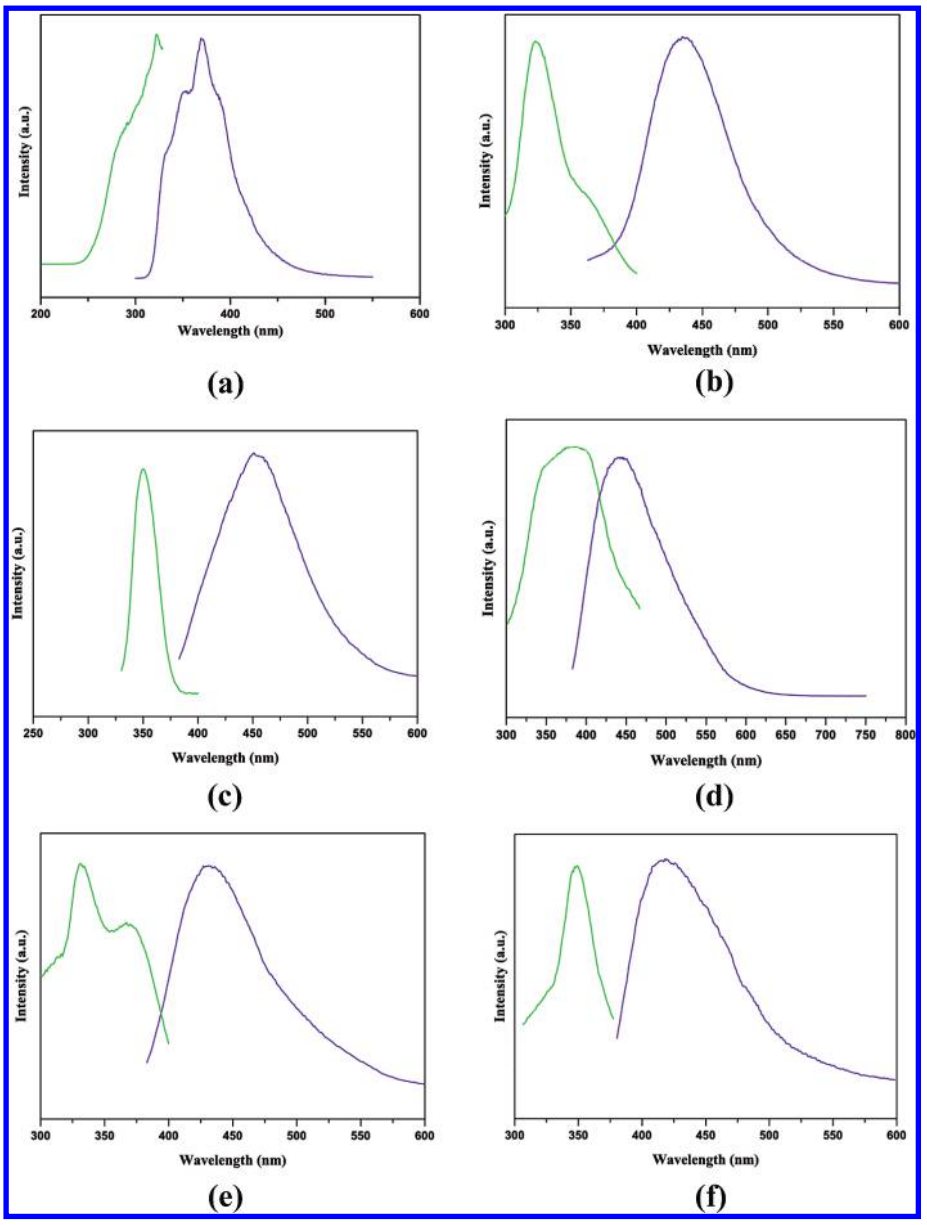

Figure 10. Emission and excitation spectra of H_4L (a), **2** (b), **3** (c), **4** (d), **5** (e), and **6** (f).

(obsd 22.4%; calcd 29.73%). The TGA curve of **6** shows that the first weight loss in the range of 30−89 °C corresponds to the departure of an ethanol molecule (obsd 4.3%; calcd 3.24%). The second weight loss of 4.8% (calcd 5.06%) in the temperature range of 89−261 °C can be assigned to the release of two solvent water molecules. The third weight loss in the temperature range of 261−333 °C can be attributed to the removal of the coordinated water (obsd 2.3%; calcd 2.53%), and then the structure decomposed. The departure of the structure finally leads to the formation of CdO (obsd 34.8%; calcd 36.34%). The anhydrous compound **7** collapsed from 216 to 585 °C, and finally CuO was formed (obsd 15.9%; calcd 16.86%). The hydrous compound **8** lost its one coordinated water molecule from 90 to 232 °C (obsd 3.0%; calcd 3.16%). The anhydrous compound was stable up to 238 °C, where the 3D framework structure began to collapse. Then CuO was formed as the remaining residue (obsd 27.1%; calcd 28.86%). **9** released its water molecule gradually from 49 to 230 °C (obsd 6.4%; calcd 6.85%). The removal of the organic components occurred in the range of 230−514 °C. The remaining residue is of 24.9%, corresponding to the formation of CuO (calcd 24.23%). However, it is difficult to determine the organic component weight losses accurately.

Luminescent Properties. The solid-state photoluminescent properties of H_4L and compounds **2**−**6** have been investigated in the solid state at room temperature. The emission and excitation peaks of **2**−**6** are shown in Figure 10. The luminescence decay cures are shown in Figure S38 in the Supporting Information.

Compounds **2**−**6** display strong fluorescence at room temperature. The photoluminescent spectrum of the H_4L ligand shows the main peak at 370 nm (λ_{ex} = 280 nm), which is probably attributable to the $\pi^* \rightarrow$ n or $\pi^* \rightarrow \pi$ transition,[30] similar to those of the reported free benzenepolycarboxylic acids. Upon complexation of the L^{4-} anion with Zn^{II} and Cd^{II} ions, the emission arising from the free H_4L was not observable. Interestingly, the

emission spectra for compound **2** shows the main peak at 435 nm (λ_{ex} = 324 nm), which is red-shifted by 65 nm with respect to the band shown by the H_4L ligand. Compared to the free ligand H_4L, compound **3** shows different luminescent properties: it exhibits a broad emission at 443 nm when excited at 350 nm. For **4**, the emission band appears at 465 nm (λ_{ex} = 350 nm), which is highly red-shifted by 95 nm. It is clear that all of the emission peaks of compounds **2**−**4** are red-shifted with respect to the free H_4L. Because the Zn^{II} and Cd^{II} ions are difficult to oxidize or to reduce because of the d^{10} configuration, the emission of these compounds is neither metal-to-ligand charge transfer nor ligand-to-metal charge transfer in nature.[31] Moreover, replacement of the hydrogen proton by Zn^{II} or Cd^{II} ions decreases the $\pi^* \rightarrow$ n or $\pi^* \rightarrow \pi$ gap of the carboxylate ligands, resulting in a red shift of the emission peaks.[32] For the reasons above, the emission can be assigned to the chelation of the carboxylate ligands to the central metals. For compound **5**, there is only one emission peak of 434 nm (λ_{ex} = 350 nm), which is similar to that of the biim-4 ligand (λ_{em} = 438 nm). Here, the carboxylate ligand almost has no contribution to the fluorescent emission, so the emission band of compound **5** can probably be attributed to the intraligand fluorescent emission.[29b,33] Compound **6** has a strong blue emission at around 420 nm (λ_{ex} = 350 nm) and is red-shifted compared to the H_4L or bpy ligand. As a result, the emission can be assigned to the chelation of the carboxylate and bpy ligands to the central ions.

The decay curves of **2**−**6** are well fitted into a single-exponential function as $I = A\exp(-t/\tau) + y_0$, suggesting only one luminescence center. The existence of only one luminescence center of compounds **5** and **6** indicates the energy transformation between the carboxylate and neutral ligands.[34] The luminescence lifetimes (τ_2 = 8.70 ns, τ_3 = 8.98 ns, τ_4 = 7.49 ns, τ_5 = 8.65 ns, and τ_6 = 6.49 ns) are much shorter than the lifetime of the emission resulting from a triplet state (>10^{-3} s), indicating an increase from the singlet state.[32,35] The nanosecond range of the lifetime in the solid state at room temperature reveals that the emission is fluorescent in nature.

Conclusion

Nine structurally different coordination polymers based on H_4L ligands have been synthesized under hydrohedral conditions and characterized by single-crystal X-ray diffraction. **1** displays a rare trinodal (3,4,7)-connected net, while the 3D structure of **2** can be simplified to α-Po topology net. When the pH values were tuned, two different frameworks of compounds **3** and **4** were obtained. Both **3** and **4** possess pentanuclear Zn^{II} clusters. However, **3** displays a complex 3D framework, whereas **4** demonstrates a scarce 3D porous framework with discrete $[Zn(H_2O)_6]^{2+}$ cations occupying the channels. Compared to **3**, introduction of the biim-4 ligand into **5** leads to a rare trinodal (3,5)-conneced network with a Schläfli symbol of $(4^2\cdot6)(6^2\cdot8)(4^2\cdot6^2\cdot8^5\cdot10)$. In comparison with **2**, introduction of the bpy ligand into **6** results in a 2D Cd−L motif, which is further pillared by bpy ligands to give an unusual (4,6)-connected net. **7** and **8** were synthesized under different pH values. **7** shows a novel polythreading structure, where the H_2L^{2-} anion is partly deprotonated. Nonetheless, **8** exhibits a scarce trinodal (3,4,5)-connected self-penetrating network. Compared to **8**, the decrease of the reaction temperature of **9** results in an unprecedented tetranodal (2,4)-connected network. The investigations in this paper not only illustrate that a structural and compositional diversity of coordination polymers can be achieved by changing the pH values, the reaction temperatures, the central metals, and the neutral ligands but also provide a new example of the H_4L ligand for the design of novel frameworks and topologies. The results indicate that the pH values, reaction temperatures, central metals, and N-donor bridging ligands play important roles in the formation of coordination polymers.

Acknowledgment. We thank the Program for Changjiang Scholars and Innovative Research Teams in Chinese University, China Postdoctoral Science Foundation, the Postdoctoral Foundation of Northeast Normal University (NENU), the Training Fund of NENU's Scientific Innovation Project, and the Analysis and Testing Foundation of NENU for support.

Supporting Information Available: X-ray crystallographic files (CIF), diagrams of the structures, selected bond distances and angles, eight coordination modes of the reported 1,2,4,5-benzenetetracarboxylate anion, and TGA curves of compounds **1**−**9**. This material is available free of charge via the Internet at http://pubs.acs.org.

(30) (a) Yang, J.; Yue, Q.; Li, G.-D.; Cao, J.-J.; Li, G.-H.; Chen, J.-S. *Inorg. Chem.* **2006**, *45*, 2857. (b) Thirumurugan, A.; Natarajan, S. *J. Chem. Soc., Dalton Trans.* **2004**, 2923. (c) Zheng, X.-J.; Jin, L.-P.; Gao, S.; Lu, S. Z. *New J. Chem.* **2005**, *29*, 798. (d) Zhang, X.-J.; Jin, L.-P.; Gao, S. *Inorg. Chem.* **2004**, *43*, 1600.

(31) (a) Wen, L.; Li, Y.; Lu, Z.; Lin, J.; Duan, C.; Meng, Q. *Cryst. Growth Des.* **2006**, *6*, 530. (b) Wen, L.; Lu, Z.; Lin, J.; Tian, Z.; Zhu, H.; Meng, Q. *Cryst. Growth Des.* **2007**, *7*, 93. (c) Lin, J.-G.; Zang, S.-Q.; Tian, Z.-F.; Li, Y.-Z.; Xu, Y.-Y.; Zhu, H.-Z.; Meng, Q.-J. *CrystEngComm* **2007**, *9*, 915.

(32) Ma, J.-F.; Yang, J.; Li, S.-L.; Song, S.-Y. *Cryst. Growth Des.* **2005**, *5*, 807.

(33) (a) Zhang, L.; Qin, Y.-Y.; Li, Z.-J.; Lin, Q.-P.; Cheng, J.-K.; Zhang, J.; Yao, Y.-G. *Inorg. Chem.* **2008**, *47*, 8286. (b) Li, X.; Cao, R.; Sun, D.; Yuan, D.; Bi, W.; Li, X.; Wang, Y. *J. Mol. Struct.* **2004**, *694*, 205.

(34) Seo, S.-J.; Zhao, D.; Suh, K.; Shin, J. H.; Bae, B.-S. *J. Lumin.* **2008**, *128*, 565.

(35) (a) Li, G. Z.; Wang, Z. L.; Yu, M.; Quan, Z. W.; Lin, J. *J. Solid State Chem.* **2006**, *179*, 2698. (b) Li, G. Z.; Yu, M. Z.; Wang, L.; Lin, J.; Wang, R. S.; Fang, J. *J. Nanosci. Nanotechnol.* **2006**, *6*, 1416.